Physics Letters B 795 (2019) 281–307

Contents lists available at ScienceDirect

Physics Letters B

www.elsevier.com/locate/physletb

Measurement of electroweak WZ boson production and search for new physics in WZ + two jets events in pp collisions at $\sqrt{s} = 13$ TeV

The CMS Collaboration *

CERN, Switzerland

ARTICLE INFO

Article history:
Received 13 January 2019
Received in revised form 30 April 2019
Accepted 27 May 2019
Available online 31 May 2019
Editor: M. Doser

Keywords:
CMS
Physics
SM
WZ
VBS

ABSTRACT

A measurement of WZ electroweak (EW) vector boson scattering is presented. The measurement is performed in the leptonic decay modes WZ $\rightarrow \ell\nu\ell'\ell'$, where $\ell, \ell' = \mathrm{e}, \mu$. The analysis is based on a data sample of proton-proton collisions at $\sqrt{s} = 13$ TeV at the LHC collected with the CMS detector and corresponding to an integrated luminosity of 35.9 fb^{-1}. The WZ plus two jet production cross section is measured in fiducial regions with enhanced contributions from EW production and found to be consistent with standard model predictions. The EW WZ production in association with two jets is measured with an observed (expected) significance of 2.2 (2.5) standard deviations. Constraints on charged Higgs boson production and on anomalous quartic gauge couplings in terms of dimension-eight effective field theory operators are also presented.

1. Introduction

The discovery of a scalar boson with couplings consistent with those of the standard model (SM) Higgs boson (H) by the ATLAS and CMS Collaborations [1–3] at the CERN LHC provides evidence that the W and Z bosons acquire mass through the Brout-Englert-Higgs mechanism [4–9]. However, current measurements of the Higgs boson couplings [10,11] do not preclude the existence of scalar isospin doublets, triplets, or higher isospin representations alongside the single isospin doublet field responsible for breaking the electroweak (EW) symmetry in the SM [12,13]. In addition to their couplings to the Higgs boson, the non-Abelian nature of the EW sector of the SM leads to quartic and triple self-interactions of the massive vector bosons. Physics beyond the SM in the EW sector is expected to include interactions with the vector and Higgs bosons that modify their effective couplings. Characterizing the self-interactions of the vector bosons is thus of great importance.

The total WZ production cross section in proton-proton (pp) collisions has been measured in the leptonic decay modes by the ATLAS and CMS Collaborations at 7, 8, and 13 TeV [14–18], and limits on anomalous triple gauge couplings [19] are presented in Refs. [15,17,20]. Constraints on anomalous quartic gauge couplings (aQGC) [21] are presented by the ATLAS Collaboration at 8 TeV in Ref. [15]. At the LHC, quartic WZ interactions are accessible through triple vector boson production or via vector boson scattering (VBS), where vector bosons are radiated from the incoming quarks before interacting, as illustrated in Fig. 1 (upper left). The VBS processes form a distinct experimental signature characterized by the W and Z bosons with two forward, high-momentum jets, arising from the hadronization of two quarks. They are part of an important subclass of processes contributing to WZ plus two jet (WZjj) production that proceeds via the EW interaction at tree level, $\mathcal{O}(\alpha^4)$, referred to as EW-induced WZjj production, or simply EW WZ production. An additional contribution to the WZjj state proceeds via quantum chromodynamics (QCD) radiation of partons from an incoming quark or gluon, shown in Fig. 1 (upper right), leading to tree-level contributions at $\mathcal{O}(\alpha^2\alpha_S^2)$. This class of processes is referred to as QCD-induced WZjj production (or QCD WZ).

The first study of EW WZ production at the LHC was performed by the ATLAS Collaboration at 8 TeV [15]. A measurement at 13 TeV with an observed statistical significance for the EW WZ process greater than 5 standard deviations has recently been reported and submitted for publication by the ATLAS Collaboration [22]. This letter reports searches for EW WZ production in the SM and for new physics modifying the WWZZ coupling in pp collisions at $\sqrt{s} = 13$ TeV. Two fiducial WZjj cross sections are presented, both in phase spaces with enhanced contributions from the EW WZ process. The data sample corresponds to an integrated luminosity of 35.9 fb^{-1} collected with the CMS detector [23] at the CERN LHC in 2016. The analysis selects events with exactly three

* *E-mail address:* cms-publication-committee-chair@cern.ch.

https://doi.org/10.1016/j.physletb.2019.05.042

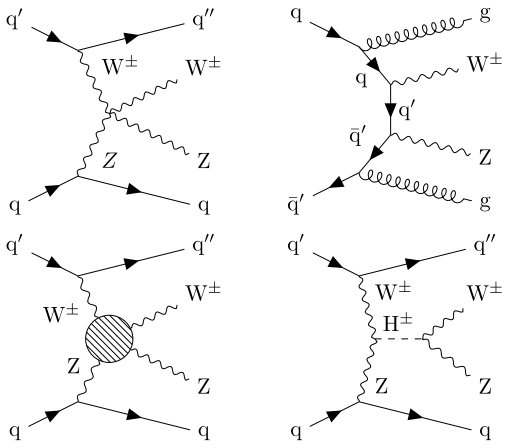

Fig. 1. Representative Feynman diagrams for WZjj production in the SM and beyond the SM. The EW-induced component of WZ production includes quartic interactions (upper left) of the vector bosons. This is distinguishable from QCD-induced production (upper right) through kinematic variables. New physics in the EW sector modifying the quartic coupling can be parameterized in terms of dimension-eight effective field theory operators (lower left). Specific models modifying this interaction include those predicting charged Higgs bosons (lower right).

leptons (electrons or muons), missing transverse momentum $p_{\mathrm{T}}^{\mathrm{miss}}$, and two jets at high pseudorapidity η with a large dijet system invariant mass m_{jj}, characteristic of VBS processes. The kinematic variables of the two forward and high momentum jets, including η separation and m_{jj}, are used to identify the EW WZ component of WZjj production. An excess of events with respect to the SM prediction could indicate contributions from additional gauge boson or vector resonances [24], charged scalar or Higgs bosons [25], or it could suggest that the gauge or Higgs bosons are not elementary [26]. We study such deviations in terms of aQGCs in the generalized framework of dimension-eight effective field theory operators, Fig. 1 (lower left), and in terms of charged Higgs bosons, Fig. 1 (lower right), and we place limits on their production cross sections and operator couplings.

2. The CMS detector

The central feature of the CMS apparatus is a superconducting solenoid of 6 m internal diameter, providing a magnetic field of 3.8 T. Within the solenoid volume are silicon pixel and strip tracking detectors, a lead tungstate crystal electromagnetic calorimeter (ECAL), and a brass and scintillator hadron calorimeter (HCAL), each composed of a barrel and two endcap sections. Forward calorimeters extend the η coverage provided by the barrel and endcap detectors up to $|\eta| < 5$. Muons are measured in gas-ionization detectors embedded in the steel flux-return yoke outside the solenoid.

Events of interest are selected using a two-level trigger system [27]. The first level of the CMS trigger system, composed of custom hardware processors, uses information from the calorimeters and muon detectors to select events of interest in a fixed time interval of 3.2 μs. The high-level trigger processor farm further decreases the event rate from around 100 kHz to less than 1 kHz, before data storage [27].

A more detailed description of the CMS detector, together with a definition of the coordinate system used and the relevant kinematic variables, can be found in Ref. [23].

3. Signal and background simulation

Several Monte Carlo (MC) event generators are used to simulate the signal and background processes.

The EW-induced production of WZ boson pairs and two final-state quarks, Fig. 1 (upper left), where the W and Z bosons decay leptonically, is simulated at leading order (LO) in perturbative QCD using MadGraph5_aMC@NLO v2.4.2 [28]. The MC simulation includes all contributions to the three-lepton final state at $\mathcal{O}(\alpha^6)$, with the condition that the mass of W boson be within 30 GeV of its on-shell value from Ref. [29]. The resonant W boson is decayed using MadSpin [30]. Triboson processes, where the WZ boson pair is accompanied by a third vector boson that decays into jets, are included in the MC simulation, but account for well below 1% of the event yield for the selections described in Section 5. Contributions with an initial-state b quark are excluded from this MC simulation since they are considered part of the tZq background process. The predictions from MadGraph5_aMC@NLO are cross-checked with LO predictions from the event generators VBFNLO 3.0 [31] and SHERPA v2.2.4 [32,33], and with fixed-order calculations from MoCaNLO+Recola [34,35]. Agreement is obtained when using equivalent configurations of input parameters, including couplings, particle masses and widths, and the choice of renormalization (μ_{R}) and factorization scales (μ_{F}).

Several MC simulations of the QCD WZ process, Fig. 1 (upper right), are considered. The simulations are inclusive in the number of jets associated with the leptonically decaying W and Z bosons, and therefore comprise the full WZjj state. The primary MC simulation is simulated at LO with MadGraph5_aMC@NLO v2.4.2, with contributions to WZ production with up to three outgoing partons included in the matrix element calculation. The different jet multiplicities are merged using the MLM scheme [36]. A next-to-leading order (NLO) MC simulation from MadGraph5_aMC@NLO v2.3.3 with zero or one outgoing partons at Born level, merged using the FxFx scheme [37], and an inclusive NLO simulation from POWHEG 2.0 [38–41] are also utilized. The LO MC simulation with MLM merging, referred to as the MLM-merged simulation, is used as the central prediction for the analysis because of its inclusion of WZ plus three-parton contributions at tree level, which are relevant to WZjj production. The other MC simulations, used to assess the modeling uncertainty in the QCD WZ process, are referred to as the FxFx-merged and the POWHEG simulations, respectively. Each MC simulation is normalized to the NLO cross section from POWHEG 2.0.

In addition to the EW WZ and QCD WZ processes, which at tree level are $\mathcal{O}(\alpha^4)$ and $\mathcal{O}(\alpha^2\alpha_S^2)$ respectively, a smaller contribution at $\mathcal{O}(\alpha^3\alpha_S)$ contributes to the WZjj state. We refer to this contribution as the interference term. It is evaluated using MC simulations of particle-level events generated with MadGraph5_aMC@NLO v2.6.0. The process is simulated with the dynamic μ_{R} and μ_{F} set to the maximum outgoing quark p_{T} per event, and with fixed scales $\mu_{\mathrm{R}} = \mu_{\mathrm{F}} = m_{\mathrm{W}}$, where m_{W} is the world average value of the W boson mass, taken from Ref. [29].

The associated production of a Z boson and a single top quark, referred to as tZq production, is simulated at NLO in the four-flavor scheme using MadGraph5_aMC@NLO v2.3.3. The MC simulation is normalized using a cross section computed at NLO with MadGraph5_aMC@NLO in the five-flavor scheme, following the procedure of Ref. [42]. The production of Z boson pairs via $\mathrm{q\bar{q}}$ annihilation is generated at NLO in perturbative QCD with POWHEG 2.0 while the $\mathrm{gg} \to \mathrm{ZZ}$ process is simulated at LO with MCFM 7.0 [43]. The ZZ simulations are normalized to the cross section calculated at next-to-next-to-leading order for $\mathrm{q\bar{q}} \to \mathrm{ZZ}$ with MATRIX [44, 45] (K factor 1.1) and at NLO for $\mathrm{gg} \to \mathrm{ZZ}$ [46] (K factor 1.7). The EW production of Z boson pairs and two final-state quarks, where the Z bosons decay leptonically, is simulated at LO using MadGraph5_aMC@NLO v2.3.3. Background from $\mathrm{Z}\gamma$, $\mathrm{t\bar{t}V}$ ($\mathrm{t\bar{t}W}$, $\mathrm{t\bar{t}Z}$), and triboson events VVV (WWZ, WZZ, ZZZ) are generated at NLO

with MadGraph5_aMC@NLO v2.3.3, with the vector bosons generated on-shell and decayed via MadSpin.

The simulation of the aQGC processes is performed at LO using MadGraph5_aMC@NLO v2.4.2 and employs matrix element reweighting to obtain a finely spaced grid of parameters for each of the anomalous couplings operators probed by the analysis. The configuration of input parameters is equivalent to that used for the EW WZ simulation described previously. The production of charged Higgs bosons in the Georgi–Machacek (GM) model [47] is simulated at LO using MadGraph5_aMC@NLO v2.3.3 and normalized using the next-to-next-to-leading order cross sections reported in Ref. [48].

The pythia v8.212 [49,50] package is used for parton showering, hadronization, and underlying event simulation, with parameters set by the CUETP8M1 tune [51] for all simulated samples. For the EW WZ process, comparisons are made at particle-level with the parton shower and hadronization of sherpa and with herwig v7.1 [52,53]. For all MC simulations used in this analysis, the NNPDF3.0 [54] set of parton distribution functions (PDFs) is used, with PDFs calculated to the same order in perturbative QCD as the hard scattering process.

The detector response is simulated using a detailed description of the CMS detector implemented in the Geant4 package [55,56]. The simulated events are reconstructed using the same algorithms used for the data. The simulated samples include additional interactions in the same and neighboring bunch crossings, referred to as pileup. Simulated events are weighted so the pileup distribution reproduces that observed in the data, which has an average of about 23 interactions per bunch crossing.

4. Event reconstruction

In this analysis, the particle-flow (PF) event reconstruction algorithm [57] is used. The PF algorithm aims to reconstruct and identify each individual particle as a physics object in an event, with an optimized combination of information from the various elements of the CMS detector. The energy of photons is obtained from the ECAL measurement. The energy of electrons is determined from a combination of the electron momentum at the primary interaction vertex as determined by the tracker, the energy of the corresponding ECAL cluster, and the energy sum of all bremsstrahlung photons spatially compatible with originating from the electron track. The energy of muons is obtained from the curvature of the corresponding track. The energy of charged hadrons is determined from a combination of their momentum measured in the tracker and the matching ECAL and HCAL energy deposits, corrected for zero-suppression effects and for the response function of the calorimeters to hadronic showers. Finally, the energy of neutral hadrons is obtained from the corresponding corrected ECAL and HCAL energies.

The reconstructed vertex with the largest value of summed physics-object p_{T}^2 (where p_{T} is the transverse momentum) is the primary pp interaction vertex. The physics objects are the jets, clustered using a jet finding algorithm [58,59] with the tracks assigned to the vertex as inputs, and the associated $p_{\mathrm{T}}^{\mathrm{miss}}$, taken as the negative vector sum of the $p_{\mathrm{T}}^{\mathrm{j}}$ of those jets.

Electrons are reconstructed within the geometrical acceptance $|\eta^{\mathrm{e}}| < 2.5$. The reconstruction combines the information from clusters of energy deposits in the ECAL and the trajectory in the tracker [60]. To reduce the electron misidentification rate, electron candidates are subjected to additional identification criteria based on the distribution of the electromagnetic shower in the ECAL, the relative amount of energy deposited in the HCAL, a matching of the trajectory of an electron track with the cluster in the ECAL, and its consistency with originating from the selected primary vertex. Candidates that are identified as originating from photon conversions in the detector material are removed.

Muons are reconstructed within $|\eta^{\mu}| < 2.4$ [61]. The reconstruction combines the information from both the tracker and the muon spectrometer. The muons are selected from among the reconstructed muon track candidates by applying minimal quality requirements on the track components in the muon system and by ensuring that muons are associated with small energy deposits in the calorimeters.

For each lepton track, the distance of closest approach to the primary vertex in the transverse plane is required to be less than 0.05 (0.10) cm for electrons in the barrel (endcap) region and 0.02 cm for muons. The distance along the beamline must be less than 0.1 (0.2) cm for electrons in the barrel (endcap) and 0.1 cm for muons.

Jets are reconstructed using PF objects. The anti-k_{T} jet clustering algorithm [58] with a distance parameter $R = 0.4$ is used. To exclude electrons and muons from the jet sample, the jets are required to be separated from the identified leptons by $\Delta R = \sqrt{(\Delta\eta)^2 + (\Delta\phi)^2} > 0.4$, where ϕ is the azimuthal angle in radians. The CMS standard method for jet energy corrections [62] is applied. These include corrections to the pileup contribution that keep the jet energy correction and the corresponding uncertainty almost independent of the number of pileup interactions. In order to reject jets coming from pileup collisions (pileup jets), a multivariate-based jet identification algorithm [63] is applied. This algorithm takes advantage of differences in the shape of energy deposits in a jet cone between jets from hard-scattering and from pileup interactions. The jets are required to have $p_{\mathrm{T}}^{\mathrm{j}} > 30$ GeV and $|\eta^{\mathrm{j}}| < 4.7$. We identify potential top quark backgrounds by identifying the b quark produced in its decay via the combined secondary vertex b-tagging algorithm with the *tight* working point [64]. The efficiency for selecting b quark jets is ≈49% with a misidentification probability of ≈4% for c quark jets and ≈0.1% for light-quark and gluon jets.

The isolation of individual electrons or muons is defined relative to their p_{T}^{ℓ} by summing over the p_{T} of charged hadrons and neutral particles within a cone with radius $\Delta R < 0.3$ (0.4) around the electron (muon) direction at the interaction vertex:

$$I^{\ell} = \left(\sum p_{\mathrm{T}}^{\mathrm{charged}} + \max\left[0, \sum p_{\mathrm{T}}^{\mathrm{neutral}} + \sum p_{\mathrm{T}}^{\gamma} - p_{\mathrm{T}}^{\mathrm{PU}}\right] \right) \Big/ p_{\mathrm{T}}^{\ell}.$$

Here, $\sum p_{\mathrm{T}}^{\mathrm{charged}}$ is the scalar p_{T} sum of charged hadrons originating from the primary vertex. The $\sum p_{\mathrm{T}}^{\mathrm{neutral}}$ and $\sum p_{\mathrm{T}}^{\gamma}$ are the scalar p_{T} sums for neutral hadrons and photons, respectively. The neutral contribution to the isolation from pileup events, $p_{\mathrm{T}}^{\mathrm{PU}}$, is estimated differently for electrons and muons. For electrons, $p_{\mathrm{T}}^{\mathrm{PU}} \equiv \rho A_{\mathrm{eff}}$, where the average transverse momentum flow density ρ is calculated in each event using the "jet area" method [65], which defines ρ as the median of the ratio of the jet transverse momentum to the jet area, $p_{\mathrm{T}}^{\mathrm{j}}/A_{\mathrm{j}}$, for all pileup jets in the event. The effective area A_{eff} is the geometric area of the isolation cone times an η-dependent correction factor that accounts for the residual dependence of the isolation on the pileup. For muons, $p_{\mathrm{T}}^{\mathrm{PU}} \equiv 0.5 \sum_i p_{\mathrm{T}}^{\mathrm{PU},i}$, where i runs over the charged hadrons originating from pileup vertices and the factor 0.5 corrects for the ratio of charged to neutral particle contributions in the isolation cone. Electrons are considered isolated if $I^{\mathrm{e}} < 0.036, (0.094)$ for the barrel (endcap) region, whereas muons are considered isolated if $I^{\mu} < 0.15$, where the values are optimized for aggressive background rejection while maintaining a reconstruction efficiency of ≈70%. Relaxed identification criteria are defined by $I^{\mu} < 0.40$ for muons and by relaxed track quality and detector-based isolation

for electrons. The overall efficiencies of the reconstruction, identification, and isolation requirements for the prompt e or μ are measured in data and simulation in bins of p_{T}^{ℓ} and $|\eta^{\ell}|$ using a "tag-and-probe" technique [66] applied to an inclusive sample of Z events. The data to simulation efficiency ratios are used as scale factors to correct the simulated event yields.

5. Event selection

Collision events are selected by triggers that require the presence of one or two electrons or muons. The p_{T}^{ℓ} threshold for the single lepton trigger is 25 (20) GeV for the electron (muon) trigger. For the dilepton triggers, with the same or different flavors, the minimum p_{T}^{ℓ} of the leading and subleading leptons are 17 (17) and 12 (8) GeV for electrons (muons), respectively. The combination of these trigger paths brings the trigger efficiency for selected three-lepton events to nearly 100%. Partial mistiming of signals in the forward region of the electromagnetic calorimeter (ECAL) endcaps ($2.5 < |\eta| < 3.0$) led to early readout for a significant fraction of events with forward jet activity, and a corresponding reduction in the level 1 trigger efficiency. A correction for this effect is determined in bins of jet $p_{\mathrm{T}}^{\mathrm{j}}$ and η^{j} using an unbiased data sample. This loss of efficiency is about 1% for m_{jj} of 200 GeV, increasing to about 15% for $m_{\mathrm{jj}} > 2$ TeV.

A selected event is required to have three lepton candidates $\ell\ell'\ell'$, where $\ell, \ell' = \mathrm{e}, \mu$. All leptons must pass the identification and isolation requirements described in Section 4. The electrons and muons can be directly produced from a W or Z boson decay or from a W or Z boson with an intermediate τ lepton decay. The $\ell'\ell'$ pair consists of two leptons with opposite charge and the same flavor, as expected for a Z boson candidate. One of the leptons from the Z boson candidate is required to have $p_{\mathrm{T}}^{\ell'_1} > 25$ GeV and the other $p_{\mathrm{T}}^{\ell'_2} > 15$ GeV. For events with three same-flavor leptons, two oppositely charged, same-flavor combinations are possible. The pair with invariant mass closest to $m_{\mathrm{Z}} = 91.2$ GeV, the nominal Z boson mass from Ref. [29], is selected as the Z boson candidate. The remaining lepton is associated with the W boson and must have $p_{\mathrm{T}}^{\ell} > 20$ GeV. Events containing additional leptons satisfying the relaxed identification criteria with $p_{\mathrm{T}}^{\ell} > 10$ GeV are rejected. Because of the neutrino in the final state, the events are required to have $p_{\mathrm{T}}^{\mathrm{miss}} > 30$ GeV. To reduce contributions from $\mathrm{t\bar{t}}$ events, the leptons constituting the Z boson candidate are required to have an invariant mass satisfying $|m_{\ell'\ell'} - m_{\mathrm{Z}}| < 15$ GeV and events with a b tagged jet with $p_{\mathrm{T}}^{\mathrm{b}} > 30$ GeV and $|\eta^{\mathrm{b}}| < 2.4$ are vetoed.

The invariant mass of any dilepton pair $m_{\ell\ell}$ must be greater than 4 GeV. Such a requirement is necessary in theoretical calculations to avoid divergences from collinear emission of same-flavor opposite-sign dilepton pairs, and 4 GeV is chosen to avoid low mass resonances. The selection is extended to all dilepton pairs to reduce contributions from backgrounds with soft leptons while having a negligible effect on signal efficiency. The trilepton invariant mass, $m_{3\ell}$, is required to be more than 100 GeV to exclude a region where production of Z bosons with final-state photon radiation is expected to contribute.

Furthermore, the event must have at least two jets with $p_{\mathrm{T}}^{\mathrm{j}} > 50$ GeV and $|\eta^{\mathrm{j}}| < 4.7$. The jet with the highest $p_{\mathrm{T}}^{\mathrm{j}}$ is called the leading jet and the jet with the second-highest $p_{\mathrm{T}}^{\mathrm{j}}$ the subleading jet. To exploit the unique signature of the VBS process, these two jets are required to have $m_{\mathrm{jj}} > 500$ GeV and η separation $|\Delta\eta(\mathrm{j}_1, \mathrm{j}_2)| \equiv |\Delta\eta_{\mathrm{jj}}| > 2.5$. The variable $\eta^*_{3\ell} = \eta^{3\ell} - (\eta^{\mathrm{j}_1} + \eta^{\mathrm{j}_2})/2$ of the three-lepton system is additionally required to be between -2.5 and 2.5. This selection is referred to as the "EW signal selection." The same set of selections, but with no requirement on $\eta^*_{3\ell}$ and with the relaxed requirement $p_{\mathrm{T}}^{j} > 30$ GeV, is used in searches for charged Higgs bosons and therefore called the "Higgs boson selection." A summary of these selections is shown in Table 1.

Table 1
Summary of event selections and fiducial region definitions for the analysis. The selections labeled "EW signal" and "Higgs boson" are applied to data and reconstructed simulated events. The EW signal selection is used for all measurements except for the charged Higgs boson search that uses the selection indicated in the column labeled "Higgs boson." The WZjj cross section is reported in the fiducial regions defined by the selections specified in the last two columns applied to particle-level simulated events. The variables n_{j} and n_{b} refer to the number of anti-k_{T} jets and the number of anti-k_{T} b-tagged jets, respectively. Other variables are defined in the text.

	EW signal	Higgs boson	Tight fiducial	Loose fiducial
$p_{\mathrm{T}}^{\ell'_1}$ [GeV]	>25	>25	>25	>20
$p_{\mathrm{T}}^{\ell'_2}$ [GeV]	>15	>15	>15	>20
p_{T}^{ℓ} [GeV]	>20	>20	>20	>20
$\lvert\eta^{\mu}\rvert$	<2.4	<2.4	<2.5	<2.5
$\lvert\eta^{\mathrm{e}}\rvert$	<2.5	<2.5	<2.5	<2.5
$\lvert m_{\ell'\ell'} - m_{\mathrm{Z}}\rvert$ [GeV]	<15	<15	<15	<15
$m_{3\ell}$ [GeV]	>100	>100	>100	>100
$m_{\ell\ell}$ [GeV]	>4	>4	>4	>4
$p_{\mathrm{T}}^{\mathrm{miss}}$ [GeV]	>30	>30	–	–
$\lvert\eta^{\mathrm{j}}\rvert$	< 4.7	<4.7	<4.7	<4.7
$p_{\mathrm{T}}^{\mathrm{j}}$ [GeV]	>50	>30	>50	>30
$\lvert\Delta R(\mathrm{j}, \ell)\rvert$	>0.4	>0.4	>0.4	>0.4
n_{j}	≥2	≥2	≥2	≥2
$p_{\mathrm{T}}^{\mathrm{b}}$ [GeV]	>30	>30	–	–
$\lvert\eta^{\mathrm{b}}\rvert$	<2.4	<2.4	–	–
n_{b}	=0	=0	–	–
m_{jj}	>500	>500	>500	>500
$\lvert\Delta\eta_{\mathrm{jj}}\rvert$	>2.5	>2.5	>2.5	>2.5
$\lvert\eta^{3\ell} - (\eta^{\mathrm{j}_1} + \eta^{\mathrm{j}_2})/2\rvert$	<2.5	–	<2.5	–

Sideband regions of events with a similar topology to signal events, but outside the signal region, are used to constrain the normalization of the QCD WZ process in the EW WZ measurement and in searches for new physics. We refer to this region as the "QCD WZ sideband region." It consists of events with $m_{\mathrm{jj}} > 100$ GeV satisfying all requirements applied to signal events, but failing at least one of the signal discriminating variables, i.e., $m_{\mathrm{jj}} < 500$ GeV or $|\Delta\eta_{\mathrm{jj}}| < 2.5$. For the EW WZ measurement, events satisfying $|\eta^*_{3\ell}| > 2.5$ are also selected in the sideband region.

To reduce the dependence on theoretical predictions, measurements are reported in two fiducial regions, defined in Table 1. The "tight fiducial region" is defined to be as close as possible to the measurement phase space, whereas the "loose fiducial region" is designed to be easily reproducible in theoretical calculations or in MC simulations, following the procedure of Ref. [34]. The fiducial predictions are defined through selections on particle-level simulated events using the Rivet [67] framework, which provides a toolkit for analyzing simulated events in a model-independent way. Electrons and muons are required to be prompt (i.e., not from hadron decays), and those produced in the decay of a τ lepton are not considered in the definition of the fiducial phase space. The momenta of prompt photons located within a cone of radius $\Delta R = 0.1$ are added to the lepton momentum to correct for final-state photon radiation, referred to as "dressing." The three highest p_{T} leptons are selected and associated with the W and Z bosons with the same procedure used in the data selection. The fiducial cross section in the QCD WZ sideband region is defined following the tight fiducial region of Table 1, with $m_{\mathrm{jj}} > 100$ GeV and $m_{\mathrm{jj}} < 500$ GeV or $|\Delta\eta_{\mathrm{jj}}| < 2.5$ or $|\eta^*_{3\ell}| > 2.5$. Theoretical predictions are evaluated using MadGraph5_aMC@NLO at LO interfaced to pythia with the samples described in Section 3.

6. Background estimation

Background contributions in this analysis are divided into two categories: background processes with prompt isolated leptons, e.g., ZZ, tZq, $t\bar{t}Z$; and background processes with nonprompt leptons from hadrons decaying to leptons inside jets or jets misidentified as isolated leptons, primarily $t\bar{t}$ and Z+jets. The background processes with prompt leptons are estimated from MC simulation, whereas backgrounds with nonprompt leptons from hadronic activity are estimated from data using control samples. The nonprompt component of the $Z\gamma$ process, in which the photon experiences conversion into leptons in the tracker, is evaluated using MC simulation.

The contribution from QCD WZ production is estimated with MC simulation. It is considered signal for the WZjj cross section measurement, but is the dominant background for the EW WZ measurement and in searches for new physics. For the EW WZ measurement and new physics searches, the normalization of the QCD WZ process is constrained by data in the QCD WZ sideband region. The cross section predicted by the MLM-merged sample in the QCD WZ sideband region is $18.6^{+2.9}_{-2.3}$ (scale) $\pm$ 1.0 (PDF) fb, where the scale and PDF uncertainties are calculated using the procedure described in Section 7. In this region the normalization correction, which is derived from a fit to the data, is consistent with unity. The EW WZ process, considered signal for the WZjj and EW WZ measurements but background to new physics searches, is also estimated using MC simulation.

The contribution from background processes with nonprompt leptons is evaluated with data control samples of events satisfying relaxed lepton identification requirements using the technique described in Refs. [16,68]. Events satisfying the full analysis selection, with the exception that one, two, or three leptons pass relaxed identification requirements but fail the more stringent requirements applied to signal events, are selected to form relaxed lepton control samples. These control samples are mutually independent and, additionally, independent from the signal selection. The small contribution to the relaxed lepton control samples from events with three prompt leptons is estimated with MC simulation and subtracted from the event samples.

The expected contribution in the signal region is estimated using "loose-to-tight" efficiency factors applied to the lepton candidates failing the analysis requirements in the control region events. The efficiency factors are calculated from a sample of $Z + \ell_{\text{cand}}$ events, where Z denotes a pair of oppositely charged, same-flavor leptons satisfying the full identification requirements and $|m_{\ell^+\ell^-} - m_Z| < 10$ GeV, and ℓ_{cand} is a lepton candidate satisfying the relaxed identification. The loose-to-tight efficiency factors are obtained from ratios of events where the ℓ_{cand} object satisfies the full identification requirements to events where all identification criteria are not satisfied, and is parameterized as a function of p_T and η. A cross-check of the technique is performed by repeating the procedure with efficiency factors derived from a sample of events dominated by dijet production. The loose-to-tight efficiency factors obtained in the two regions agree to within 30% for the full p_T and η range.

This method is validated in nonoverlapping data samples enriched in Drell–Yan and $t\bar{t}$ contributions. The Drell–Yan sample is defined by inverting the selection requirement in p_T^{miss}, and the $t\bar{t}$ sample is defined by requiring at least one b-tagged jet and rejecting events with $|m_{\ell'\ell'} - m_Z| < 5$ GeV while keeping all other requirements for the signal region. The predictions derived from the relaxed lepton data control samples agree with the measurements in the Drell–Yan and $t\bar{t}$ data samples to within 20%.

The small size of the loose lepton control samples and $Z\gamma$ MC simulation limit differential predictions in the EW signal region. Therefore, the combined shape of the estimated nonprompt and $Z\gamma$ backgrounds for both electrons and muons are used as background for the EW WZ measurement and in the extraction of constraints on aQGCs. The normalization of the distributions per channel are taken from the ratio of the nonprompt ($Z\gamma$) yield in a single channel to the total nonprompt ($Z\gamma$) event yield measured in WZjj events with no requirements on the dijet system. These ratios are consistent within the statistical uncertainty with ratios measured when relaxing the jet p_T requirement in WZjj events, in WZ events inclusive in the number of jets, and in events satisfying the EW signal and QCD WZ sideband selections.

7. Systematic uncertainties

The dominant uncertainties in both the cross section measurement and new physics searches are those associated with the jet energy scale (JES) and resolution (JER). The JES and JER uncertainties are evaluated in simulated events by smearing and scaling the relevant observables and propagating the effects to the event selection and the kinematic variables used in the analysis. The uncertainty in the event yield in the EW signal selection due to the JES and JER is 9% for QCD WZ and 5% for EW WZ processes. For the QCD WZ (EW WZ) process, the JES uncertainty varies in the range of 5–25% (3–15%) with increasing values of m_{jj} and $|\Delta\eta_{jj}|$.

The uncertainties in signal and background processes estimated with MC simulation are evaluated from the theoretical uncertainties of the predictions. Event weights in the MC simulations are used to evaluate variations of the central prediction. Scale uncertainties are estimated by independently varying μ_R and μ_F by a factor of two from their nominal values, with the condition that $1/2 \leq \mu_R/\mu_F \leq 2$. The maximal and minimal variations are obtained per bin to form a shape-dependent variation band. The PDF uncertainties are evaluated by combining the predictions per bin from the fit and α_s variations of the NNPDF3.0 set according to the procedure described in Ref. [69] for MC replica sets. The scale and PDF uncertainties are uncorrelated for different signal and background process and 100% correlated across bins for the distributions used to extract results. For MC simulations normalized to a cross section computed at a higher order in QCD, the uncertainties are calculated from the order of the MC simulation.

The uncertainty in modeling the EW WZ and QCD WZ processes has a large impact in the EW WZ measurement. In addition to the uncertainties from scale and PDF choice, comparisons of alternative matrix element and parton shower generators are considered. The uncertainty in the QCD WZ process is derived by comparing the predictions of the MLM-merged simulation and those obtained with the FxFx-merged simulation, after fixing the normalization to the observed data in the QCD WZ sideband region. Differences between the predictions of the MC simulations in the signal region and in the ratio of the QCD WZ sideband to the signal region event yields are considered in the comparisons. The differences in predictions are generally within the scale and PDF uncertainties of the MC simulations, and a 10% normalization uncertainty is assigned to account for the observed discrepancies. The results obtained using the POWHEG simulation, which predicts a slightly softer m_{jj} spectrum, are also largely contained within the theoretical uncertainties considered. However, because WZjj events from this simulation arise from soft radiation from the parton shower, it is not explicitly considered in the uncertainty evaluation. For the EW WZ process, the MC simulations described in Section 3 agree within the theoretical uncertainties from the PDF and the choice of μ_R and μ_F for the kinematic variables considered in the analysis, so no additional uncertainty is assigned.

The interference term is evaluated on particle-level simulated events selected from the MC simulations described in Section 3.

It is positive, and roughly 12% of the EW WZ contribution in the QCD WZ sideband region and 4% in the EW signal region for both MC simulations considered, consistent with the results reported in Ref. [34]. The ratio of the interference to the EW WZ decreases with increasing m_{jj}, consistent with the observations of Refs. [34, 70]. These values are used as a symmetric shape uncertainty in the EW WZ prediction. This uncertainty is lower than other theoretical uncertainties and has a negligible contribution to the uncertainty in the EW WZ measurement.

Higher-order EW corrections in VBS processes are known to be negative and at the level of tens of percent, with the correction increasing in magnitude with increasing m_{jj} and m_{VV} [71]. We do not apply corrections to the WZjj MC simulation, but we have verified that the significance of the EW WZ measurement is insensitive to higher-order EW corrections by performing the signal extraction described in Section 8 with the m_{jj} predicted by the EW WZ MC simulation modified by the corrections from Ref. [72]. As the relative effect of the EW corrections on SM and anomalous WZjj production is unknown, we do not apply corrections to the SM backgrounds or new physics signals for our results. Because corrections to the SM WZjj production that decrease the expected number of events at high m_{WZ} lead to more stringent limits on new physics, this is a conservative approach.

The uncertainties related to the finite number of simulated events, or to the limited number of events in data control regions, affect the signal and background predictions. They are uncorrelated across different samples, and across bins of a single distribution. The limited number of events in the relaxed lepton control samples used for the nonprompt background estimate is the dominant contribution to this uncertainty.

The nonprompt background estimate is also affected by systematic uncertainties from the jet flavor composition of the relaxed lepton control samples and loose-to-tight extrapolation factors. The systematic uncertainty in the nonprompt event yield is 30% for both electrons and muons, uncorrelated between channels. It covers the largest difference observed between the estimated and measured numbers of events in data control samples enriched in $t\bar{t}$ and Drell–Yan contributions and the differences between using extrapolation factors derived in Z+jet and dijet events.

Systematic uncertainties are less than 1% for the trigger efficiency and 1–3% for the lepton identification and isolation requirements, depending on the lepton flavors. Other systematic uncertainties are related to the use of simulated samples: 1% for the effects of pileup and 1–2% for the p_T^{miss} reconstruction, estimated by varying the energies of the PF objects within their uncertainties. The uncertainty in the b tagging efficiency is 2% for WZ events, which accounts for differences in b tagging efficiencies between MC simulations and data. The uncertainty in the integrated luminosity of the data sample is 2.5% [73]. This uncertainty affects both the signal and the simulated portion of the background estimation, but does not affect the background estimation from data.

For the extraction of results, log-normal probability density functions are assumed for the nuisance parameters affecting the event yields of the various background contributions, whereas systematic uncertainties that affect the shape of the distributions are represented by nuisance parameters whose variation results in a continuous perturbation of the spectrum [74] and are assumed to have a Gaussian probability density function. A summary of the contribution of each systematic uncertainty to the total WZjj cross section measurement is presented in Table 2. The impact of each systematic uncertainty in the WZjj cross section measurement is obtained by freezing the set of associated nuisance parameters to their best-fit values and comparing the total uncertainty in the signal strength to the result from the nominal fit. The prompt background normalization uncertainty includes the scale and PDF uncertainties in the background processes estimated using MC simulations.

Table 2
The dominant systematic uncertainty contributions in the fiducial WZjj cross section measurement.

Source of syst. uncertainty	Relative uncertainty in σ_{WZjj} [%]
Jet energy scale	+11/−8.1
Jet energy resolution	+1.9/−2.1
Prompt background normalization	+2.2/−2.2
Nonprompt normalization	+2.5/−2.5
Nonprompt event count	+6.0/−5.8
Lepton energy scale and eff.	+3.5/−2.7
b tagging	+2.0/−1.7
Integrated luminosity	+3.6/−3.0

8. Fiducial WZjj cross section measurement and search for EW WZ production

The cross section for WZjj production, without separating by production mechanism, is measured with a combined maximum likelihood fit to the observed event yields for the EW signal selection. The likelihood is a combination of individual likelihoods for the four leptonic decay channels (eee, eeμ, $\mu\mu$e, $\mu\mu\mu$) for the signal and background hypotheses with the statistical and systematic uncertainties in the form of nuisance parameters. To minimize the dependence of the result on theoretical predictions, the likelihood function is built from the event yields per channel without considering information about the distribution of events in kinematic variables. The expected event yields for the EW- and QCD-induced WZjj processes are taken from the MadGraph5_aMC@NLO v2.4.2 predictions. The WZjj signal strength μ_{WZjj}, which is the ratio of the measured signal yield to the expected number of signal events, is treated as a free parameter in the fit.

The best-fit value for the WZjj signal strength is used to obtain a cross section in the tight fiducial region defined in Table 1. The measured fiducial WZjj cross section in this region is

$$\sigma_{WZjj}^{fid} = 3.18^{+0.57}_{-0.52}\,(stat)^{+0.43}_{-0.36}\,(syst)\,fb = 3.18^{+0.71}_{-0.63}\,fb.$$

This result can be compared with the predicted value of $3.27^{+0.39}_{-0.32}$ (scale) $\pm$ 0.15 (PDF) fb. The EW WZ and QCD WZ contributions are calculated independently from the samples described in Section 3 and their uncertainties are combined in quadrature to obtain the WZjj cross section prediction. The predicted EW WZ cross section is $1.25^{+0.11}_{-0.09}$ (scale) $\pm$ 0.06 (PDF) fb, and the interference term contribution in this region is less than 1% of the total cross section.

Results are also obtained in a looser fiducial region, defined in Table 1 following Ref. [34], to simplify comparisons with theoretical calculations. The acceptance from the loose to tight fiducial region is (72.4 $\pm$ 0.8)%, computed using MadGraph5_aMC@NLO interfaced to pythia. The uncertainty in the acceptance is evaluated by combining the scale and PDF uncertainties in the EW WZ and QCD WZ predictions in quadrature. The scale uncertainty in the QCD WZ contribution is the dominant component of the uncertainty. The resulting WZjj loose fiducial cross section is

$$\sigma_{WZjj}^{fid,loose} = 4.39^{+0.78}_{-0.72}\,(stat)^{+0.60}_{-0.50}\,(syst)\,fb = 4.39^{+0.98}_{-0.87}\,fb,$$

compared with the predicted value of $4.51^{+0.59}_{-0.45}$ (scale) $\pm$ 0.18 (PDF) fb. The EW WZ and QCD WZ contributions and their uncertainties are treated independently with the same approach as described for the tight fiducial region. The predicted EW WZ cross section in the loose region is $1.48^{+0.13}_{-0.11}$ (scale) $\pm$ 0.07 (PDF) fb, and the relative contribution from the interference term is less the 1%.

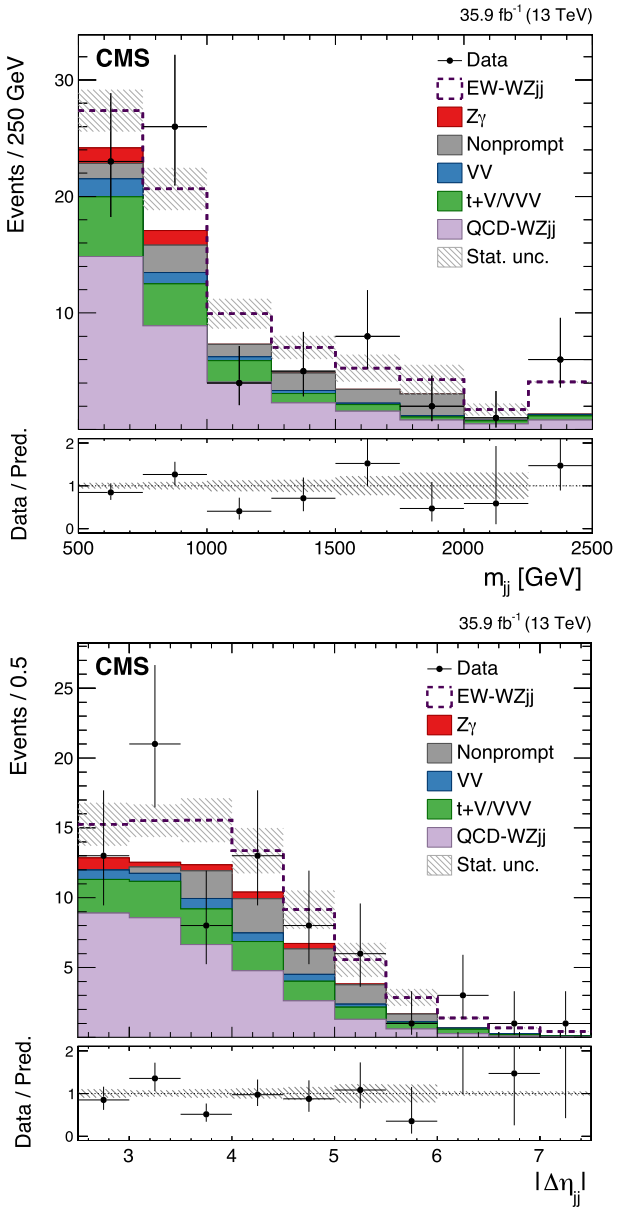

Fig. 2. The m_{jj} (upper) and $|\Delta\eta_{jj}|$ (lower) of the two leading jets for events satisfying the EW signal selection. The last bin contains all events with $m_{jj} > 2500$ GeV (upper) and $|\Delta\eta_{jj}| > 7.5$ (lower). The dashed line shows the expected EW WZ contribution stacked on top of the backgrounds that are shown as filled histograms. The hatched bands represent the total and relative statistical uncertainties on the predicted yields. The bottom panel shows the ratio of the number of events measured in data to the total number of expected events. The predicted yields are shown with their pre-fit normalizations.

Separating the EW- and QCD-induced components of WZjj events requires exploiting the different kinematic signatures of the two processes. The relative fraction of the EW WZ process with respect to the QCD WZ process and other backgrounds grows with increasing values of the m_{jj} and $|\Delta\eta_{jj}|$ of the leading jets, as demonstrated in Fig. 2. This motivates the use of a 2D distribution built from these variables for the extraction of the EW WZ signal via a maximum likelihood fit. This 2D distribution, shown as a one-dimensional histogram in Fig. 3, along with the yield in the QCD WZ sideband region, are combined in a binned likelihood involving the expected and observed numbers of events in each bin. The likelihood is a combination of individual likelihoods for the four decay channels.

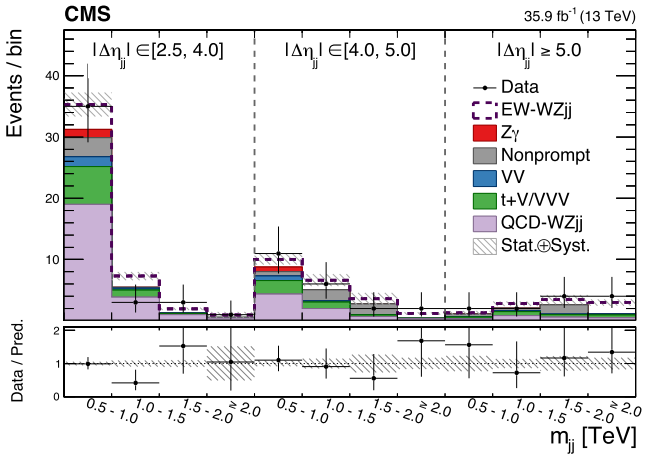

Fig. 3. The one-dimensional representation of the 2D distribution of m_{jj} and $|\Delta\eta_{jj}|$, used for the EW signal extraction. The x axis shows the m_{jj} distribution in the indicated bins, split into three bins of $\Delta\eta_{jj}$: $\Delta\eta_{jj} \in [2.5, 4], [4, 5], \geq 5$. The dashed line represents the EW WZ contribution stacked on top of the backgrounds that are shown as filled histograms. The hatched bands represent the total and relative systematic uncertainties on the predicted yields. The bottom panel shows the ratio of the number of events measured in data to the total number of expected events. The predicted yields are shown with their best-fit normalizations.

The systematic uncertainties are represented by nuisance parameters that are allowed to vary according to their probability density functions, and correlation across bins and between different sources of uncertainty is taken into account. The expected number of signal events is taken from the MadGraph5_aMC@NLO v2.4.2 prediction at LO, multiplied by a signal strength μ_{EW} which is treated as a free parameter in the fit.

The best-fit value for the signal strength μ_{EW} is

$$\mu_{EW} = 0.82^{+0.51}_{-0.43},$$

consistent with the SM expectation at LO of $\mu_{EW,\,LO} = 1$, with respect to the predicted cross section for the EW WZ process in the tight fiducial region. The significance of the signal is quantified by calculating the local p-value for an upward fluctuation of the data relative to the background prediction using a profile likelihood ratio test statistic and asymptotic formulae [75]. The observed (expected) statistical significance for EW WZ production is 2.2 (2.5) standard deviations. A modification to the predicted cross section used in the fit trivially rescales the signal strength but does not impact the significance of the result. The total uncertainty of the measurement is dominated by the statistical uncertainty of the data. The post-fit yields for the signal and background corresponding to the best-fit signal strength for EW WZ production are shown in Table 3.

9. Limits on anomalous quartic gauge couplings

Events satisfying the EW signal selection are used to constrain aQGCs in the effective field theory approach [76]. Results are obtained following the formulation of Ref. [21] that proposes nine independent dimension-eight operators, which assume the SU(2)×U(1) symmetry of the EW gauge sector as well as the presence of an SM Higgs boson. All operators are charge conjugation and parity-conserving. The WZjj channel is most sensitive to the T0, T1, and T2 operators that are constructed purely from the SU(2) gauge fields, the S0 and S1 operators that involve interactions with the Higgs field, and the M0 and M1 operators that involve a mixture of gauge and Higgs field interactions.

Table 3
Post-fit event yields after the signal extraction fit to events satisfying the EW signal selection. The EW WZ process is corrected for the observed value of μ_{EW}.

Process	$\mu\mu\mu$	$\mu\mu$e	eeμ	eee	Total yield
QCD WZ	13.5 ± 0.8	9.1 ± 0.5	6.8 ± 0.4	4.6 ± 0.3	34.1 ± 1.1
t+V/VVV	5.6 ± 0.4	3.1 ± 0.2	2.5 ± 0.2	1.7 ± 0.1	12.9 ± 0.5
Nonprompt	5.2 ± 2.0	2.4 ± 0.9	1.5 ± 0.6	0.7 ± 0.3	9.8 ± 2.3
VV	0.8 ± 0.1	1.6 ± 0.2	0.4 ± 0.0	0.7 ± 0.1	3.5 ± 0.2
Zγ	0.3 ± 0.1	1.2 ± 0.8	<0.1	0.6 ± 0.2	2.2 ± 0.8
Pred. background	25.5 ± 2.1	17.4 ± 1.5	11.2 ± 0.8	8.3 ± 0.6	62.4 ± 2.8
EW WZ signal	6.0 ± 1.2	4.2 ± 0.8	2.9 ± 0.6	2.1 ± 0.4	15.1 ± 1.6
Data	38	15	12	10	75

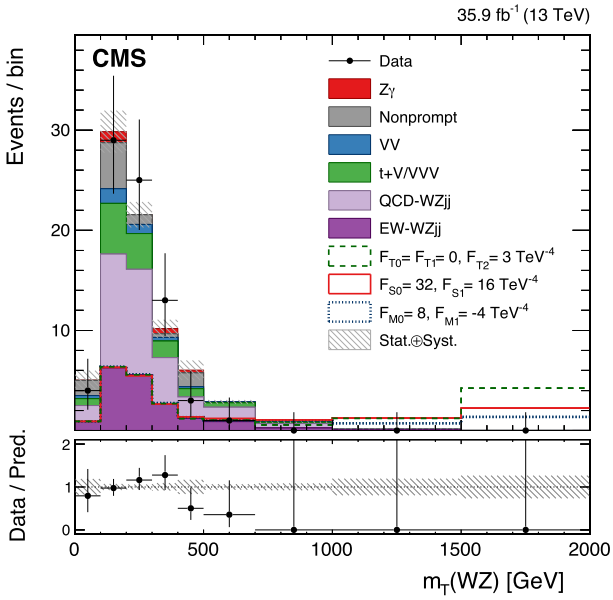

Fig. 4. m_T(WZ) for events satisfying the EW signal selection, used to place constraints on the anomalous coupling parameters. The dashed lines show predictions for several aQGC parameters values that modify the EW WZ process. The last bin contains all events with m_T(WZ) > 2000 GeV. The hatched bands represent the total and relative systematic uncertainties on the predicted yields. The bottom panel shows the ratio of the number of events measured in data to the total number of expected events. The predicted yields are shown with their best-fit normalizations from the background-only fit.

The presence of nonzero aQGCs would enhance the production of events with high WZ mass. This motivates the use of the transverse mass of the WZ system, defined as

$$m_T(WZ) = \sqrt{[E_T(W) + E_T(Z)]^2 - \left[\vec{p}_T(W) + \vec{p}_T(Z)\right]^2},$$

with $E_T = \sqrt{m^2 + p_T^2}$, where the W candidate is constructed from the $\vec{p}_T^{\,miss}$ and the lepton associated with the W boson, and m is the invariant mass of the W or Z candidate, to constrain the parameters $f_{\mathcal{O}i}/\Lambda^4$. In this formulation, $f_{\mathcal{O}i}$ is a dimensionless coefficient for the operator $\mathcal{O}_i$ and Λ is the energy scale of new physics. The m_T(WZ) for events satisfying the EW signal selection is shown in Fig. 4. The predictions of several indicative aQGC operators and coefficients are also shown.

The MC simulations of nonzero aQGCs include the SM EW WZ process, with an increase in the yield at high m_T(WZ) arising from parameters different from their SM values. Because the increase of the expected yield over the SM prediction exhibits a quadratic dependence on the operator coefficient, a parabolic function is fitted to the predicted yields per bin to obtain a smooth interpolation between the discrete operator coefficients considered in the MC simulation. The one-dimensional 95% confidence level (CL) limits are extracted using the CL_s criterion [77,78,75], with all parameters except for the coefficient being probed set to zero. The SM prediction, including the EW WZ process, is treated as the null hypothesis. The expected prompt backgrounds are normalized to the predictions of the MC simulations, with no corrections applied for the results of the EW WZ or WZjj measurements. No deviation from the SM prediction is observed, and the resulting observed and expected limits are summarized in Table 4.

Table 4
Observed and expected 95% CL limits for each operator coefficient (in TeV^{-4}) while all other parameters are set to zero.

Parameters	Exp. limit	Obs. limit
f_{M0}/Λ^4	[−11.2, 11.6]	[−9.15, 9.15]
f_{M1}/Λ^4	[−10.9, 11.6]	[−9.15, 9.45]
f_{S0}/Λ^4	[−32.5, 34.5]	[−26.5, 27.5]
f_{S1}/Λ^4	[−50.2, 53.2]	[−41.2, 42.8]
f_{T0}/Λ^4	[−0.87, 0.89]	[−0.75, 0.81]
f_{T1}/Λ^4	[−0.56, 0.60]	[−0.49, 0.55]
f_{T2}/Λ^4	[−1.78, 2.00]	[−1.49, 1.85]

Constraints are also placed on aQGC parameters using a two-dimensional scan, where two parameters are probed in the fit with all others set to zero. This approach is motivated by correlations between operators and physical couplings, and for comparisons with alternative formulations of dimension-eight operators. In particular, the quartic gauge interactions of the massive gauge bosons is a function of S0 and S1, while combinations of the M0 and M1 operators can be compared with the formulation of Ref. [79]. The resulting 2D 95% CL intervals for these parameters are shown in Fig. 5.

10. Limits on charged Higgs boson production

Theories with Higgs sectors including SU(2) triplets can give rise to charged Higgs bosons ($H^\pm$) with large couplings to the vector bosons of the SM. A prominent one is the GM model [47], where the Higgs sector is extended by one real and one complex SU(2) triplet to preserve custodial symmetry at tree level for arbitrary vacuum expectation values. In this model, the couplings of $H^\pm$ and the vector bosons depend on $m(H^\pm)$ and the parameter $\sin\theta_H$, or s_H, which represents the mixing angle of the vacuum expectation values in the model, and determines the fraction of the W and Z boson masses generated by the vacuum expectation values of the triplets. This analysis extends the previous study of $H^\pm$ production via vector boson fusion by the CMS Collaboration in the same channel [68].

A combined fit of the predicted signal and background yields to the data in the Higgs boson selection is performed in bins of m_T(WZ), simultaneously with the event yield in the QCD WZ sideband region, to derive model-independent expected and observed upper limits on $\sigma(H+jj)(H^\pm)\,\mathcal{B}(H^\pm \to WZ)$ at 95% CL using the CL_s criterion. The distribution and binning of the m_T(WZ) distribution used in the fit are shown in Fig. 6. The upper limits as a function of $m(H^\pm)$ are shown in Fig. 7 (upper). The results assume that the intrinsic width of the $H^\pm$ is $\lesssim 0.05 m(H^\pm)$, which is below the experimental resolution in the phase space considered.

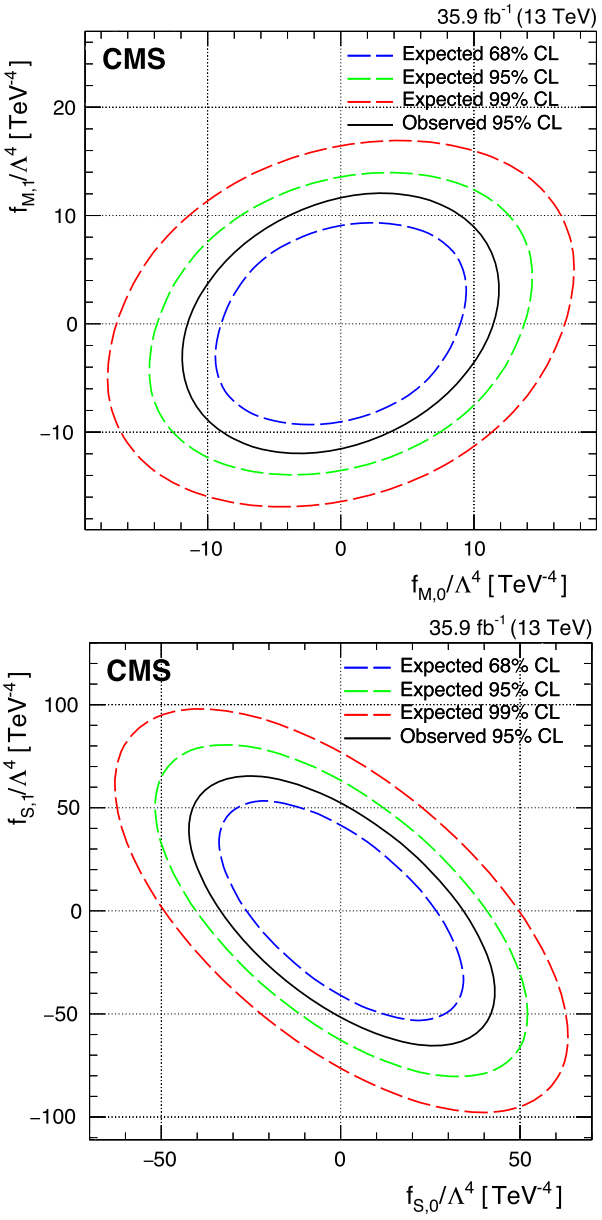

Fig. 5. Two-dimensional observed 95% CL intervals (solid contour) and expected 68, 95, and 99% CL intervals (dashed contour) on the selected aQGC parameters. The values of coefficients outside of contours are excluded at the corresponding CL.

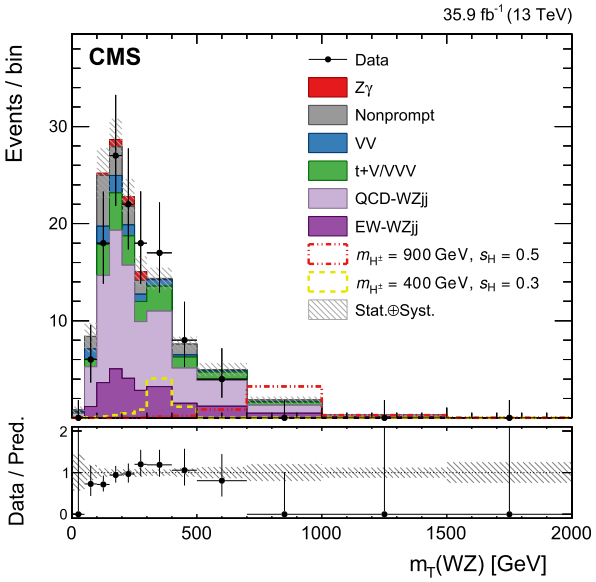

Fig. 6. m_{T}(WZ) for events satisfying the Higgs boson selection, used to place constraints on the production of charged Higgs bosons. The last bin contains all events with $m_{\mathrm{T}}(\mathrm{WZ}) > 2000$ GeV. The dashed lines show predictions from the GM model with $m(\mathrm{H}^{\pm}) = 400$ (900) GeV and $s_{\mathrm{H}} = 0.3$ (0.5). The bottom panel shows the ratio of the number of events measured in data to the total number of expected events. The hatched bands represent the total and relative systematic uncertainties on the predicted background yields. The predicted yields are shown with their best-fit normalizations from the background-only fit.

The model-independent upper limits are compared with the predicted cross sections at next-to-next-to-leading order in the GM model in the s_{H}-$m(\mathrm{H}^{\pm})$ plane, under the assumptions defined for the "H5plane" in Ref. [48]. For the probed parameter space and m_{T}(WZ) distribution used for signal extraction, the varying width as a function of s_{H} is assumed to have negligible effect on the result. The value of the branching fraction $\mathcal{B}(\mathrm{H}^{\pm} \to \mathrm{WZ})$ is assumed to be unity. In Fig. 7 (lower), the excluded s_{H} values as a function of $m(\mathrm{H}^{\pm})$ are shown. The blue shaded region shows the parameter space for which the $\mathrm{H}^{\pm}$ total width exceeds 10% of $m(\mathrm{H}^{\pm})$, where the model is not applicable because of perturbativity and vacuum stability requirements [48].

11. Summary

A measurement of the production of a W and a Z boson in association with two jets has been presented, using events where both bosons decay leptonically. Results are based on data corresponding to an integrated luminosity of 35.9 fb^{-1} recorded in proton-proton collisions at $\sqrt{s} = 13$ TeV with the CMS detector at the LHC in 2016. The cross section in a tight fiducial region with enhanced contributions from electroweak (EW) WZ production is $\sigma^{\mathrm{fid}}_{\mathrm{WZjj}} = 3.18^{+0.71}_{-0.63}$ fb, consistent with the standard model (SM) prediction. The dijet mass and dijet rapidity separation are used to measure the signal strength of EW WZ production with respect to the SM expectation, resulting in $\mu_{\mathrm{EW}} = 0.82^{+0.51}_{-0.43}$. The significance of this result is 2.2 standard deviations with 2.5 standard deviations expected.

Constraints are placed on anomalous quartic gauge couplings in terms of dimension-eight effective field theory operators, and upper limits are given on the production cross section times branching fraction of charged Higgs bosons. The upper limits on charged Higgs boson production via vector boson fusion with decay to a W and a Z boson extend the results previously published by the CMS Collaboration [68] and are comparable to those of the ATLAS Collaboration [80]. These are the first limits for dimension-eight effective field theory operators in the WZ channel at 13 TeV.

Acknowledgements

We congratulate our colleagues in the CERN accelerator departments for the excellent performance of the LHC and thank the technical and administrative staffs at CERN and at other CMS institutes for their contributions to the success of the CMS effort. In addition, we gratefully acknowledge the computing centers and personnel of the Worldwide LHC Computing Grid for delivering so effectively the computing infrastructure essential to our analyses. Finally, we acknowledge the enduring support for the construction and operation of the LHC and the CMS detector provided by the following funding agencies: BMBWF and FWF (Austria); FNRS and FWO (Belgium); CNPq, CAPES, FAPERJ, FAPERGS, and FAPESP (Brazil); MES (Bulgaria); CERN; CAS, MoST, and NSFC (China); COLCIENCIAS (Colombia); MSES and CSF (Croatia); RPF

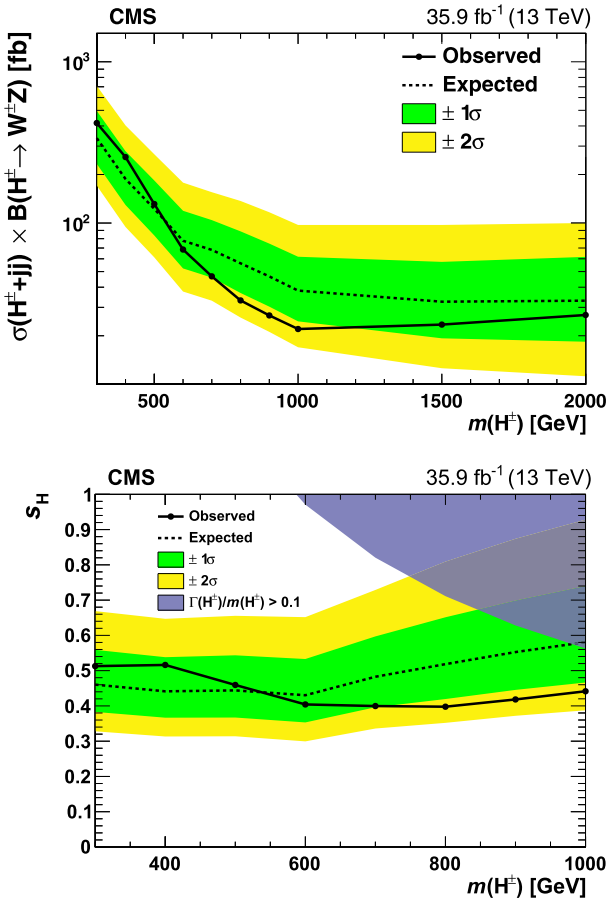

Fig. 7. Expected (dashed lines) and observed (solid lines) upper limits at 95% CL for the model independent $\sigma(\mathrm{H}^{\pm})\,\mathcal{B}(H^{\pm} \to \mathrm{W}^{\pm}\mathrm{Z})$ as a function of $m(\mathrm{H}^{\pm})$ (upper) and for s_{H} as a function of m_{H} in the GM model (lower). The blue shaded area covers the theoretically not allowed parameter space [48].

(Cyprus); SENESCYT (Ecuador); MoER, ERC IUT, and ERDF (Estonia); Academy of Finland, MEC, and HIP (Finland); CEA and CNRS/IN2P3 (France); BMBF, DFG, and HGF (Germany); GSRT (Greece); NKFIA (Hungary); DAE and DST (India); IPM (Iran); SFI (Ireland); INFN (Italy); MSIP and NRF (Republic of Korea); MES (Latvia); LAS (Lithuania); MOE and UM (Malaysia); BUAP, CINVESTAV, CONACYT, LNS, SEP, and UASLP-FAI (Mexico); MOS (Montenegro); MBIE (New Zealand); PAEC (Pakistan); MSHE and NSC (Poland); FCT (Portugal); JINR (Dubna); MON, RosAtom, RAS, RFBR, and NRC KI (Russia); MESTD (Serbia); SEIDI, CPAN, PCTI, and FEDER (Spain); MOSTR (Sri Lanka); Swiss Funding Agencies (Switzerland); MST (Taipei); ThEPCenter, IPST, STAR, and NSTDA (Thailand); TUBITAK and TAEK (Turkey); NASU and SFFR (Ukraine); STFC (United Kingdom); DOE and NSF (USA).

Rachada-pisek Individuals have received support from the Marie-Curie program and the European Research Council and Horizon 2020 Grant, contract No. 675440 (European Union); the Leventis Foundation; the A.P. Sloan Foundation; the Alexander von Humboldt Foundation; the Belgian Federal Science Policy Office; the Fonds pour la Formation à la Recherche dans l'Industrie et dans l'Agriculture (FRIA-Belgium); the Agentschap voor Innovatie door Wetenschap en Technologie (IWT-Belgium); the F.R.S.-FNRS and FWO (Belgium) under the "Excellence of Science – EOS" – be.h project n. 30820817; the Ministry of Education, Youth and Sports (MEYS) of the Czech Republic; the Lendület ("Momentum") Programme and the János Bolyai Research Scholarship of the Hungarian Academy of Sciences, the New National Excellence Program ÚNKP, the NKFIA research grants 123842, 123959, 124845, 124850, and 125105 (Hungary); the Council of Science and Industrial Research, India; the HOMING PLUS programme of the Foundation for Polish Science, cofinanced from European Union, Regional Development Fund, the Mobility Plus programme of the Ministry of Science and Higher Education, the National Science Center (Poland), contracts Harmonia 2014/14/M/ST2/00428, Opus 2014/13/B/ST2/02543, 2014/15/B/ST2/03998, and 2015/19/B/ST2/02861, Sonata-bis 2012/07/E/ST2/01406; the National Priorities Research Program by Qatar National Research Fund; the Programa Estatal de Fomento de la Investigación Científica y Técnica de Excelencia María de Maeztu, grant MDM-2015-0509 and the Programa Severo Ochoa del Principado de Asturias; the Thalis and Aristeia programmes cofinanced by EU-ESF and the Greek NSRF; the Rachadapisek Sompot Fund for Postdoctoral Fellowship, Chulalongkorn University and the Chulalongkorn Academic into Its 2nd Century Project Advancement Project (Thailand); the Welch Foundation, contract C-1845; and the Weston Havens Foundation (USA).

References

[1] ATLAS Collaboration, Observation of a new particle in the search for the standard model Higgs boson with the ATLAS detector at the LHC, Phys. Lett. B 716 (2012) 1, https://doi.org/10.1016/j.physletb.2012.08.020, arXiv:1207.7214.

[2] CMS Collaboration, Observation of a new boson at a mass of 125 GeV with the CMS experiment at the LHC, Phys. Lett. B 716 (2012) 30, https://doi.org/10.1016/j.physletb.2012.08.021, arXiv:1207.7235.

[3] CMS Collaboration, Observation of a new boson with mass near 125 GeV in pp collisions at $\sqrt{s} = 7$ and 8 TeV, J. High Energy Phys. 06 (2013) 081, https://doi.org/10.1007/JHEP06(2013)081, arXiv:1303.4571.

[4] F. Englert, R. Brout, Broken symmetry and the mass of gauge vector mesons, Phys. Rev. Lett. 13 (1964) 321, https://doi.org/10.1103/PhysRevLett.13.321.

[5] P.W. Higgs, Broken symmetries, massless particles and gauge fields, Phys. Lett. 12 (1964) 132, https://doi.org/10.1016/0031-9163(64)91136-9.

[6] P.W. Higgs, Broken symmetries and the masses of gauge bosons, Phys. Rev. Lett. 13 (1964) 508, https://doi.org/10.1103/PhysRevLett.13.508.

[7] G.S. Guralnik, C.R. Hagen, T.W.B. Kibble, Global conservation laws and massless particles, Phys. Rev. Lett. 13 (1964) 585, https://doi.org/10.1103/PhysRevLett.13.585.

[8] P.W. Higgs, Spontaneous symmetry breakdown without massless bosons, Phys. Rev. 145 (1966) 1156, https://doi.org/10.1103/PhysRev.145.1156.

[9] T.W.B. Kibble, Symmetry breaking in non-Abelian gauge theories, Phys. Rev. 155 (1967) 1554, https://doi.org/10.1103/PhysRev.155.1554.

[10] ATLAS and CMS Collaborations, Measurements of the Higgs boson production and decay rates and constraints on its couplings from a combined ATLAS and CMS analysis of the LHC pp collision data at $\sqrt{s} = 7$ and 8 TeV, J. High Energy Phys. 08 (2016) 045, https://doi.org/10.1007/JHEP08(2016)045, arXiv:1606.02266.

[11] CMS Collaboration, Combined measurements of Higgs boson couplings in proton-proton collisions at $\sqrt{s} = 13$ TeV, Eur. Phys. J. C 79 (2019) 421, https://doi.org/10.1140/epjc/s10052-019-6909-y, arXiv:1809.10733.

[12] C.-W. Chiang, G. Cottin, O. Eberhardt, Global fits in the Georgi-Machacek model, Phys. Rev. D 99 (2019) 015001, https://doi.org/10.1103/PhysRevD.99.015001, arXiv:1807.10660.

[13] D. Chowdhury, O. Eberhardt, Update of global two-Higgs-doublet model fits, J. High Energy Phys. 05 (2018) 161, https://doi.org/10.1007/JHEP05(2018)161, arXiv:1711.02095.

[14] ATLAS Collaboration, Measurement of WZ production in proton-proton collisions at $\sqrt{s} = 7$ TeV with the ATLAS detector, Eur. Phys. J. C 72 (2012) 2173, https://doi.org/10.1140/epjc/s10052-012-2173-0, arXiv:1208.1390.

[15] ATLAS Collaboration, Measurements of $\mathrm{W}^{\pm}\mathrm{Z}$ production cross sections in pp collisions at $\sqrt{s} = 8$ TeV with the ATLAS detector and limits on anomalous gauge boson self-couplings, Phys. Rev. D 93 (2016) 092004, https://doi.org/10.1103/PhysRevD.93.092004, arXiv:1603.02151.

[16] CMS Collaboration, Measurement of the WZ production cross section in pp collisions at $\sqrt{s} = 13$ TeV, Phys. Lett. B 766 (2017) 268, https://doi.org/10.1016/j.physletb.2017.01.011, arXiv:1607.06943.

[17] CMS Collaboration, Measurement of the WZ production cross section in pp collisions at $\sqrt{s} = 7$ and 8 TeV and search for anomalous triple gauge couplings at $\sqrt{s} = 8$ TeV, Eur. Phys. J. C 77 (2017) 236, https://doi.org/10.1140/epjc/s10052-017-4730-z, arXiv:1609.05721.

[18] ATLAS Collaboration, Measurement of $\mathrm{W}^{\pm}\mathrm{Z}$ production cross sections and gauge boson polarisation in pp collisions at $\sqrt{s} = 13$ TeV with the ATLAS detector, Eur. Phys. J. C (2019), in press, arXiv:1902.05759.

[19] K. Hagiwara, J. Woodside, D. Zeppenfeld, Measuring the WWZ coupling at the Tevatron, Phys. Rev. D 41 (1990) 2113, https://doi.org/10.1103/PhysRevD.41.2113.

[20] CMS Collaboration, Measurements of the pp→WZ inclusive and differential production cross section and constraints on charged anomalous triple gauge couplings at $\sqrt{s} = 13$ TeV, J. High Energy Phys. 04 (2019) 122, https://doi.org/10.1007/JHEP04(2019)122, arXiv:1901.03428.

[21] O.J.P. Éboli, M.C. Gonzalez-Garcia, J.K. Mizukoshi, pp → jj $e^{\pm}\mu^{\pm}\nu\nu$ and jj $e^{\pm}\mu^{\mp}\nu\nu$ at $\mathcal{O}(\alpha_{em}^6)$ and $\mathcal{O}(\alpha_{em}^4\alpha_s^2)$ for the study of the quartic electroweak gauge boson vertex at CERN LHC, Phys. Rev. D 74 (2006) 073005, https://doi.org/10.1103/PhysRevD.74.073005, arXiv:hep-ph/0606118.

[22] ATLAS Collaboration, Observation of electroweak $W^{\pm}Z$ boson pair production in association with two jets in pp collisions at $\sqrt{s} = 13$ TeV with the ATLAS detector, Phys. Lett. B 793 (2019) 469, https://doi.org/10.1016/j.physletb.2019.05.012, arXiv:1812.09740.

[23] CMS Collaboration, The CMS experiment at the CERN LHC, J. Instrum. 3 (2008) S08004, https://doi.org/10.1088/1748-0221/3/08/S08004.

[24] R.L. Delgado, A. Dobado, D. Espriu, C. Garcia-Garcia, M.J. Herrero, X. Marcano, J.J. Sanz-Cillero, Production of vector resonances at the LHC via WZ-scattering: a unitarized EChL analysis, J. High Energy Phys. 11 (2017) 098, https://doi.org/10.1007/JHEP11(2017)098, arXiv:1707.04580.

[25] W. Kilian, T. Ohl, J. Reuter, M. Sekulla, Resonances at the LHC beyond the Higgs boson: the scalar/tensor case, Phys. Rev. D 93 (2016) 036004, https://doi.org/10.1103/PhysRevD.93.036004, arXiv:1511.00022.

[26] C. Csaki, C. Grojean, J. Terning, Alternatives to an elementary Higgs, Rev. Mod. Phys. 88 (2016) 045001, https://doi.org/10.1103/RevModPhys.88.045001, arXiv:1512.00468.

[27] CMS Collaboration, The CMS trigger system, J. Instrum. 12 (2017) P01020, https://doi.org/10.1088/1748-0221/12/01/P01020, arXiv:1609.02366.

[28] J. Alwall, R. Frederix, S. Frixione, V. Hirschi, F. Maltoni, O. Mattelaer, H.-S. Shao, T. Stelzer, P. Torielli, M. Zaro, The automated computation of tree-level and next-to-leading order differential cross sections, and their matching to parton shower simulations, J. High Energy Phys. 07 (2014) 079, https://doi.org/10.1007/JHEP07(2014)079, arXiv:1405.0301.

[29] M. Tanabashi, et al., Particle Data Group, Review of particle physics, Phys. Rev. D 98 (2018) 030001, https://doi.org/10.1103/PhysRevD.98.030001.

[30] P. Artoisenet, R. Frederix, O. Mattelaer, R. Rietkerk, Automatic spin-entangled decays of heavy resonances in Monte Carlo simulations, J. High Energy Phys. 03 (2013) 015, https://doi.org/10.1007/JHEP03(2013)015, arXiv:1212.3460.

[31] K. Arnold, et al., VBFNLO: a parton level Monte Carlo for processes with electroweak bosons, Comput. Phys. Commun. 180 (2009) 1661, https://doi.org/10.1016/j.cpc.2009.03.006, arXiv:0811.4559.

[32] T. Gleisberg, S. Höche, F. Krauss, M. Schönherr, S. Schumann, F. Siegert, J. Winter, Event generation with SHERPA 1.1, J. High Energy Phys. 02 (2009) 007, https://doi.org/10.1088/1126-6708/2009/02/007, arXiv:0811.4622.

[33] T. Gleisberg, S. Höche, F. Krauss, A. Schälicke, S. Schumann, J.-C. Winter, SHERPA 1.α, a proof-of-concept version, J. High Energy Phys. 02 (2004) 056, https://doi.org/10.1088/1126-6708/2004/02/056, arXiv:hep-ph/0311263.

[34] J. Bendavid, et al., Les Houches 2017: physics at TeV colliders standard model working group report, URL, https://inspirehep.net/record/1663483/files/1803.07977.pdf, arXiv:1803.07977, 2018.

[35] S. Actis, A. Denner, L. Hofer, J.-N. Lang, A. Scharf, S. Uccirati, RECOLA: recursive computation of one-loop amplitudes, Comput. Phys. Commun. 214 (2017) 140, https://doi.org/10.1016/j.cpc.2017.01.004, arXiv:1605.01090.

[36] J. Alwall, S. Höche, F. Krauss, N. Lavesson, L. Lönnblad, F. Maltoni, M.L. Mangano, M. Moretti, C.G. Papadopoulos, F. Piccinini, S. Schumann, M. Treccani, J. Winter, M. Worek, Comparative study of various algorithms for the merging of parton showers and matrix elements in hadronic collisions, Eur. Phys. J. C 53 (2008) 473, https://doi.org/10.1140/epjc/s10052-007-0490-5, arXiv:0706.2569.

[37] R. Frederix, S. Frixione, Merging meets matching in MC@NLO, J. High Energy Phys. 12 (2012) 061, https://doi.org/10.1007/JHEP12(2012)061, arXiv:1209.6215.

[38] T. Melia, P. Nason, R. Rontsch, G. Zanderighi, W^+W^-, WZ and ZZ production in the POWHEG BOX, J. High Energy Phys. 11 (2011) 078, https://doi.org/10.1007/JHEP11(2011)078, arXiv:1107.5051.

[39] P. Nason, A new method for combining NLO QCD with shower Monte Carlo algorithms, J. High Energy Phys. 11 (2004) 040, https://doi.org/10.1088/1126-6708/2004/11/040, arXiv:hep-ph/0409146.

[40] S. Frixione, P. Nason, C. Oleari, Matching NLO QCD computations with parton shower simulations: the POWHEG method, J. High Energy Phys. 11 (2007) 070, https://doi.org/10.1088/1126-6708/2007/11/070, arXiv:0709.2092.

[41] S. Alioli, P. Nason, C. Oleari, E. Re, A general framework for implementing NLO calculations in shower Monte Carlo programs: the POWHEG BOX, J. High Energy Phys. 06 (2010) 043, https://doi.org/10.1007/JHEP06(2010)043, arXiv:1002.2581.

[42] CMS Collaboration, Measurement of the associated production of a single top quark and a Z boson in pp collisions at $\sqrt{s} = 13$ TeV, Phys. Lett. B 779 (2018) 358, https://doi.org/10.1016/j.physletb.2018.02.025, arXiv:1712.02825.

[43] J.M. Campbell, R.K. Ellis, C. Williams, Vector boson pair production at the LHC, J. High Energy Phys. 07 (2011) 18, https://doi.org/10.1007/JHEP07(2011)018, arXiv:1105.0020.

[44] F. Cascioli, T. Gehrmann, M. Grazzini, S. Kallweit, P. Maierhöfer, A. von Manteuffel, S. Pozzorini, D. Rathlev, L. Tancredi, E. Weihs, ZZ production at hadron colliders in NNLO QCD, Phys. Lett. B 735 (2014) 311, https://doi.org/10.1016/j.physletb.2014.06.056, arXiv:1405.2219.

[45] M. Grazzini, S. Kallweit, M. Wiesemann, Fully differential NNLO computations with MATRIX, Eur. Phys. J. C 78 (2018) 537, https://doi.org/10.1140/epjc/s10052-018-5771-7, arXiv:1711.06631.

[46] F. Caola, K. Melnikov, R. Röntsch, L. Tancredi, QCD corrections to ZZ production in gluon fusion at the LHC, Phys. Rev. D 92 (2015) 094028, https://doi.org/10.1103/PhysRevD.92.094028, arXiv:1509.06734.

[47] H. Georgi, M. Machacek, Doubly charged Higgs bosons, Nucl. Phys. B 262 (1985) 463, https://doi.org/10.1016/0550-3213(85)90325-6.

[48] M. Zaro, H. Logan, Recommendations for the interpretation of LHC searches for H_5^0, $H_5^{\pm}$, and $H_5^{\pm\pm}$ in vector boson fusion with decays to vector boson pairs, CERN Report LHCHXSWG-2015-001, 2015, URL, https://cds.cern.ch/record/2002500.

[49] T. Sjöstrand, S. Mrenna, P. Skands, PYTHIA 6.4 physics and manual, J. High Energy Phys. 05 (2006) 026, https://doi.org/10.1088/1126-6708/2006/05/026, arXiv:hep-ph/0603175.

[50] T. Sjöstrand, S. Ask, J.R. Christiansen, R. Corke, N. Desai, P. Ilten, S. Mrenna, S. Prestel, C.O. Rasmussen, P.Z. Skands, An introduction to PYTHIA 8.2, Comput. Phys. Commun. 191 (2015) 159, https://doi.org/10.1016/j.cpc.2015.01.024, arXiv:1410.3012.

[51] CMS Collaboration, Event generator tunes obtained from underlying event and multiparton scattering measurements, Eur. Phys. J. C 76 (2016) 155, https://doi.org/10.1140/epjc/s10052-016-3988-x, arXiv:1512.00815.

[52] J. Bellm, et al., Herwig 7.0/Herwig++ 3.0 release note, Eur. Phys. J. C 76 (2016) 196, https://doi.org/10.1140/epjc/s10052-016-4018-8, arXiv:1512.01178.

[53] M. Bähr, S. Gieseke, M.A. Gigg, D. Grellscheid, K. Hamilton, O. Latunde-Dada, S. Plätzer, P. Richardson, M.H. Seymour, A. Sherstnev, B.R. Webber, Herwig++ physics and manual, Eur. Phys. J. C 58 (2008) 639, https://doi.org/10.1140/epjc/s10052-008-0798-9, arXiv:0803.0883.

[54] R.D. Ball, et al., NNPDF, Parton distributions for the LHC run II, J. High Energy Phys. 04 (2015) 040, https://doi.org/10.1007/JHEP04(2015)040, arXiv:1410.8849.

[55] S. Agostinelli, et al., GEANT4, Geant4—a simulation toolkit, Nucl. Instrum. Methods A 506 (2003) 250, https://doi.org/10.1016/S0168-9002(03)01368-8.

[56] J. Allison, et al., GEANT4 developments and applications, IEEE Trans. Nucl. Sci. 53 (2006) 270, https://doi.org/10.1109/TNS.2006.869826.

[57] CMS Collaboration, Particle-flow reconstruction and global event description with the CMS detector, J. Instrum. 12 (2017) P10003, https://doi.org/10.1088/1748-0221/12/10/P10003, arXiv:1706.04965.

[58] M. Cacciari, G.P. Salam, G. Soyez, The anti-k_T jet clustering algorithm, J. High Energy Phys. 04 (2008) 063, https://doi.org/10.1088/1126-6708/2008/04/063, arXiv:0802.1189.

[59] M. Cacciari, G.P. Salam, G. Soyez, FastJet user manual, Eur. Phys. J. C 72 (2012) 1896, https://doi.org/10.1140/epjc/s10052-012-1896-2, arXiv:1111.6097.

[60] CMS Collaboration, Performance of electron reconstruction and selection with the CMS detector in proton-proton collisions at $\sqrt{s} = 8$ TeV, J. Instrum. 10 (2015) P06005, https://doi.org/10.1088/1748-0221/10/06/P06005, arXiv:1502.02701.

[61] CMS Collaboration, Performance of the CMS muon detector and muon reconstruction with proton-proton collisions at $\sqrt{s} = 13$ TeV, J. Instrum. 13 (2018) P06015, https://doi.org/10.1088/1748-0221/13/06/P06015, arXiv:1804.04528.

[62] CMS Collaboration, Determination of jet energy calibration and transverse momentum resolution in CMS, J. Instrum. 6 (2011) P11002, https://doi.org/10.1088/1748-0221/6/11/P11002, arXiv:1107.4277.

[63] CMS Collaboration, Pileup jet identification, CMS Physics Analysis Summary CMS-PAS-JME-13-005, 2013, URL, https://cds.cern.ch/record/1581583.

[64] CMS Collaboration, Identification of heavy-flavour jets with the CMS detector in pp collisions at 13 TeV, J. Instrum. 13 (2018) P05011, https://doi.org/10.1088/1748-0221/13/05/P05011, arXiv:1712.07158.

[65] M. Cacciari, G.P. Salam, Pileup subtraction using jet areas, Phys. Lett. B 659 (2008) 119, https://doi.org/10.1016/j.physletb.2007.09.077, arXiv:0707.1378.

[66] CMS Collaboration, Measurement of the inclusive W and Z production cross sections in pp collisions at $\sqrt{s} = 7$ TeV with the CMS experiment, J. High Energy Phys. 10 (2011) 132, https://doi.org/10.1007/JHEP10(2011)132, arXiv:1107.4789.

[67] A. Buckley, J. Butterworth, L. Lonnblad, D. Grellscheid, H. Hoeth, J. Monk, H. Schulz, F. Siegert, Rivet user manual, Comput. Phys. Commun. 184 (2013) 2803, https://doi.org/10.1016/j.cpc.2013.05.021, arXiv:1003.0694.

[68] CMS Collaboration, Search for charged Higgs bosons produced via vector boson fusion and decaying into a pair of W and Z bosons using pp collisions at $\sqrt{s} =$ 13 TeV, Phys. Rev. Lett. 119 (2017) 141802, https://doi.org/10.1103/PhysRevLett.119.141802, arXiv:1705.02942.

[69] J. Butterworth, et al., PDF4LHC recommendations for LHC Run II, J. Phys. G 43 (2016) 023001, https://doi.org/10.1088/0954-3899/43/2/023001, arXiv:1510.03865.

[70] A. Ballestrero, et al., Precise predictions for same-sign W-boson scattering at the LHC, Eur. Phys. J. C 78 (2018) 671, https://doi.org/10.1140/epjc/s10052-018-6136-y, arXiv:1803.07943.

[71] B. Biedermann, A. Denner, M. Pellen, Large electroweak corrections to vector-boson scattering at the Large Hadron Collider, Phys. Rev. Lett. 118 (2017) 261801, https://doi.org/10.1103/PhysRevLett.118.261801, arXiv:1611.02951.

[72] A. Denner, S. Dittmaier, P. Maierhöfer, M. Pellen, C. Schwan, QCD and electroweak corrections to WZ scattering at the LHC, arXiv:1904.00882, 2019.

[73] CMS Collaboration, CMS luminosity measurements for the 2016 data taking period, CMS Physics Analysis Summary CMS-PAS-LUM-17-001. Accepted for publication by J. High Energy Phys. URL: https://cds.cern.ch/record/2257069, 2017.

[74] H.B. Prosper, L. Lyons (Eds.), Proceedings, PHYSTAT 2011 Workshop on Statistical Issues Related to Discovery Claims in Search Experiments and Unfolding, CERN, CERN, Geneva, 2011, https://doi.org/10.5170/CERN-2011-006.

[75] G. Cowan, K. Cranmer, E. Gross, O. Vitells, Asymptotic formulae for likelihood-based tests of new physics, Eur. Phys. J. C 71 (2011) 1554, https://doi.org/10.1140/epjc/s10052-011-1554-0, arXiv:1007.1727.

[76] C. Degrande, N. Greiner, W. Kilian, O. Mattelaer, H. Mebane, T. Stelzer, S. Willenbrock, C. Zhang, Effective field theory: a modern approach to anomalous couplings, Ann. Phys. 335 (2013) 21, https://doi.org/10.1016/j.aop.2013.04.016, arXiv:1205.4231.

[77] T. Junk, Confidence level computation for combining searches with small statistics, Nucl. Instrum. Methods A 434 (1999) 435, https://doi.org/10.1016/S0168-9002(99)00498-2, arXiv:hep-ex/9902006.

[78] A.L. Read, Presentation of search results: the CL_s technique, J. Phys. G 28 (2002) 2693, https://doi.org/10.1088/0954-3899/28/10/313.

[79] G. Belanger, F. Boudjema, Probing quartic couplings of weak bosons through three vectors production at a 500-GeV NLC, Phys. Lett. B 288 (1992) 201, https://doi.org/10.1016/0370-2693(92)91978-I.

[80] ATLAS Collaboration, Search for resonant WZ production in the fully leptonic final state in proton-proton collisions at $\sqrt{s} = 13$ TeV with the ATLAS detector, Phys. Lett. B 787 (2018) 68, https://doi.org/10.1016/j.physletb.2018.10.021, arXiv:1806.01532.

The CMS Collaboration

A.M. Sirunyan, A. Tumasyan

Yerevan Physics Institute, Yerevan, Armenia

W. Adam, F. Ambrogi, E. Asilar, T. Bergauer, J. Brandstetter, M. Dragicevic, J. Erö, A. Escalante Del Valle, M. Flechl, R. Frühwirth [1], V.M. Ghete, J. Hrubec, M. Jeitler [1], N. Krammer, I. Krätschmer, D. Liko, T. Madlener, I. Mikulec, N. Rad, H. Rohringer, J. Schieck [1], R. Schöfbeck, M. Spanring, D. Spitzbart, W. Waltenberger, J. Wittmann, C.-E. Wulz [1], M. Zarucki

Institut für Hochenergiephysik, Wien, Austria

V. Chekhovsky, V. Mossolov, J. Suarez Gonzalez

Institute for Nuclear Problems, Minsk, Belarus

E.A. De Wolf, D. Di Croce, X. Janssen, J. Lauwers, M. Pieters, H. Van Haevermaet, P. Van Mechelen, N. Van Remortel

Universiteit Antwerpen, Antwerpen, Belgium

S. Abu Zeid, F. Blekman, J. D'Hondt, J. De Clercq, K. Deroover, G. Flouris, D. Lontkovskyi, S. Lowette, I. Marchesini, S. Moortgat, L. Moreels, Q. Python, K. Skovpen, S. Tavernier, W. Van Doninck, P. Van Mulders, I. Van Parijs

Vrije Universiteit Brussel, Brussel, Belgium

D. Beghin, B. Bilin, H. Brun, B. Clerbaux, G. De Lentdecker, H. Delannoy, B. Dorney, G. Fasanella, L. Favart, R. Goldouzian, A. Grebenyuk, A.K. Kalsi, T. Lenzi, J. Luetic, N. Postiau, E. Starling, L. Thomas, C. Vander Velde, P. Vanlaer, D. Vannerom, Q. Wang

Université Libre de Bruxelles, Bruxelles, Belgium

T. Cornelis, D. Dobur, A. Fagot, M. Gul, I. Khvastunov [2], D. Poyraz, C. Roskas, D. Trocino, M. Tytgat, W. Verbeke, B. Vermassen, M. Vit, N. Zaganidis

Ghent University, Ghent, Belgium

H. Bakhshiansohi, O. Bondu, S. Brochet, G. Bruno, C. Caputo, P. David, C. Delaere, M. Delcourt, A. Giammanco, G. Krintiras, V. Lemaitre, A. Magitteri, K. Piotrzkowski, A. Saggio, M. Vidal Marono, P. Vischia, S. Wertz, J. Zobec

Université Catholique de Louvain, Louvain-la-Neuve, Belgium

F.L. Alves, G.A. Alves, M. Correa Martins Junior, G. Correia Silva, C. Hensel, A. Moraes, M.E. Pol, P. Rebello Teles

Centro Brasileiro de Pesquisas Fisicas, Rio de Janeiro, Brazil

E. Belchior Batista Das Chagas, W. Carvalho, J. Chinellato [3], E. Coelho, E.M. Da Costa, G.G. Da Silveira [4], D. De Jesus Damiao, C. De Oliveira Martins, S. Fonseca De Souza, H. Malbouisson, D. Matos Figueiredo, M. Melo De Almeida, C. Mora Herrera, L. Mundim, H. Nogima, W.L. Prado Da Silva, L.J. Sanchez Rosas, A. Santoro, A. Sznajder, M. Thiel, E.J. Tonelli Manganote [3], F. Torres Da Silva De Araujo, A. Vilela Pereira

Universidade do Estado do Rio de Janeiro, Rio de Janeiro, Brazil

S. Ahuja [a], C.A. Bernardes [a], L. Calligaris [a], T.R. Fernandez Perez Tomei [a], E.M. Gregores [b], P.G. Mercadante [b], S.F. Novaes [a], Sandra S. Padula [a]

[a] *Universidade Estadual Paulista, São Paulo, Brazil*
[b] *Universidade Federal do ABC, São Paulo, Brazil*

A. Aleksandrov, R. Hadjiiska, P. Iaydjiev, A. Marinov, M. Misheva, M. Rodozov, M. Shopova, G. Sultanov

Institute for Nuclear Research and Nuclear Energy, Bulgarian Academy of Sciences, Sofia, Bulgaria

A. Dimitrov, L. Litov, B. Pavlov, P. Petkov

University of Sofia, Sofia, Bulgaria

W. Fang [5], X. Gao [5], L. Yuan

Beihang University, Beijing, China

M. Ahmad, J.G. Bian, G.M. Chen, H.S. Chen, M. Chen, Y. Chen, C.H. Jiang, D. Leggat, H. Liao, Z. Liu, S.M. Shaheen [6], A. Spiezia, J. Tao, Z. Wang, E. Yazgan, H. Zhang, S. Zhang [6], J. Zhao

Institute of High Energy Physics, Beijing, China

Y. Ban, G. Chen, A. Levin, J. Li, L. Li, Q. Li, Y. Mao, S.J. Qian, D. Wang

State Key Laboratory of Nuclear Physics and Technology, Peking University, Beijing, China

Y. Wang

Tsinghua University, Beijing, China

C. Avila, A. Cabrera, C.A. Carrillo Montoya, L.F. Chaparro Sierra, C. Florez, C.F. González Hernández, M.A. Segura Delgado

Universidad de Los Andes, Bogota, Colombia

B. Courbon, N. Godinovic, D. Lelas, I. Puljak, T. Sculac

University of Split, Faculty of Electrical Engineering, Mechanical Engineering and Naval Architecture, Split, Croatia

Z. Antunovic, M. Kovac

University of Split, Faculty of Science, Split, Croatia

V. Brigljevic, D. Ferencek, K. Kadija, B. Mesic, A. Starodumov [7], T. Susa

Institute Rudjer Boskovic, Zagreb, Croatia

M.W. Ather, A. Attikis, M. Kolosova, G. Mavromanolakis, J. Mousa, C. Nicolaou, F. Ptochos, P.A. Razis, H. Rykaczewski

University of Cyprus, Nicosia, Cyprus

M. Finger [8], M. Finger Jr. [8]

Charles University, Prague, Czech Republic

E. Ayala

Escuela Politecnica Nacional, Quito, Ecuador

E. Carrera Jarrin

Universidad San Francisco de Quito, Quito, Ecuador

S. Khalil [9], M.A. Mahmoud [10,11], E. Salama [11,12]

Academy of Scientific Research and Technology of the Arab Republic of Egypt, Egyptian Network of High Energy Physics, Cairo, Egypt

S. Bhowmik, A. Carvalho Antunes De Oliveira, R.K. Dewanjee, K. Ehataht, M. Kadastik, M. Raidal, C. Veelken

National Institute of Chemical Physics and Biophysics, Tallinn, Estonia

P. Eerola, H. Kirschenmann, J. Pekkanen, M. Voutilainen

Department of Physics, University of Helsinki, Helsinki, Finland

J. Havukainen, J.K. Heikkilä, T. Järvinen, V. Karimäki, R. Kinnunen, T. Lampén, K. Lassila-Perini, S. Laurila, S. Lehti, T. Lindén, P. Luukka, T. Mäenpää, H. Siikonen, E. Tuominen, J. Tuominiemi

Helsinki Institute of Physics, Helsinki, Finland

T. Tuuva

Lappeenranta University of Technology, Lappeenranta, Finland

M. Besancon, F. Couderc, M. Dejardin, D. Denegri, J.L. Faure, F. Ferri, S. Ganjour, A. Givernaud, P. Gras, G. Hamel de Monchenault, P. Jarry, C. Leloup, E. Locci, J. Malcles, G. Negro, J. Rander, A. Rosowsky, M.Ö. Sahin, M. Titov

IRFU, CEA, Université Paris-Saclay, Gif-sur-Yvette, France

A. Abdulsalam [13], C. Amendola, I. Antropov, F. Beaudette, P. Busson, C. Charlot, R. Granier de Cassagnac, I. Kucher, A. Lobanov, J. Martin Blanco, C. Martin Perez, M. Nguyen, C. Ochando, G. Ortona, P. Paganini, P. Pigard, J. Rembser, R. Salerno, J.B. Sauvan, Y. Sirois, A.G. Stahl Leiton, A. Zabi, A. Zghiche

Laboratoire Leprince-Ringuet, Ecole polytechnique, CNRS/IN2P3, Université Paris-Saclay, Palaiseau, France

J.-L. Agram [14], J. Andrea, D. Bloch, J.-M. Brom, E.C. Chabert, V. Cherepanov, C. Collard, E. Conte [14], J.-C. Fontaine [14], D. Gelé, U. Goerlach, M. Jansová, A.-C. Le Bihan, N. Tonon, P. Van Hove

Université de Strasbourg, CNRS, IPHC UMR 7178, Strasbourg, France

S. Gadrat

Centre de Calcul de l'Institut National de Physique Nucleaire et de Physique des Particules, CNRS/IN2P3, Villeurbanne, France

S. Beauceron, C. Bernet, G. Boudoul, N. Chanon, R. Chierici, D. Contardo, P. Depasse, H. El Mamouni, J. Fay, L. Finco, S. Gascon, M. Gouzevitch, G. Grenier, B. Ille, F. Lagarde, I.B. Laktineh, H. Lattaud, M. Lethuillier, L. Mirabito, S. Perries, A. Popov [15], V. Sordini, G. Touquet, M. Vander Donckt, S. Viret

Université de Lyon, Université Claude Bernard Lyon 1, CNRS-IN2P3, Institut de Physique Nucléaire de Lyon, Villeurbanne, France

T. Toriashvili [16]

Georgian Technical University, Tbilisi, Georgia

D. Lomidze

Tbilisi State University, Tbilisi, Georgia

C. Autermann, L. Feld, M.K. Kiesel, K. Klein, M. Lipinski, M. Preuten, M.P. Rauch, C. Schomakers, J. Schulz, M. Teroerde, B. Wittmer

RWTH Aachen University, I. Physikalisches Institut, Aachen, Germany

A. Albert, D. Duchardt, M. Erdmann, S. Erdweg, T. Esch, R. Fischer, S. Ghosh, A. Güth, T. Hebbeker, C. Heidemann, K. Hoepfner, H. Keller, L. Mastrolorenzo, M. Merschmeyer, A. Meyer, P. Millet, S. Mukherjee, T. Pook, M. Radziej, H. Reithler, M. Rieger, A. Schmidt, D. Teyssier, S. Thüer

RWTH Aachen University, III. Physikalisches Institut A, Aachen, Germany

G. Flügge, O. Hlushchenko, T. Kress, T. Müller, A. Nehrkorn, A. Nowack, C. Pistone, O. Pooth, D. Roy, H. Sert, A. Stahl [17]

RWTH Aachen University, III. Physikalisches Institut B, Aachen, Germany

M. Aldaya Martin, T. Arndt, C. Asawatangtrakuldee, I. Babounikau, K. Beernaert, O. Behnke, U. Behrens, A. Bermúdez Martínez, D. Bertsche, A.A. Bin Anuar, K. Borras [18], V. Botta, A. Campbell, P. Connor, C. Contreras-Campana, V. Danilov, A. De Wit, M.M. Defranchis, C. Diez Pardos, D. Domínguez Damiani, G. Eckerlin, T. Eichhorn, A. Elwood, E. Eren, E. Gallo [19], A. Geiser, J.M. Grados Luyando, A. Grohsjean, M. Guthoff, M. Haranko, A. Harb, H. Jung, M. Kasemann, J. Keaveney, C. Kleinwort, J. Knolle, D. Krücker, W. Lange, A. Lelek, T. Lenz, J. Leonard, K. Lipka, W. Lohmann [20], R. Mankel, I.-A. Melzer-Pellmann, A.B. Meyer, M. Meyer, M. Missiroli, J. Mnich, V. Myronenko, S.K. Pflitsch, D. Pitzl, A. Raspereza, P. Saxena, P. Schütze, C. Schwanenberger, R. Shevchenko, A. Singh, H. Tholen, O. Turkot, A. Vagnerini, G.P. Van Onsem, R. Walsh, Y. Wen, K. Wichmann, C. Wissing, O. Zenaiev

Deutsches Elektronen-Synchrotron, Hamburg, Germany

R. Aggleton, S. Bein, L. Benato, A. Benecke, V. Blobel, T. Dreyer, A. Ebrahimi, E. Garutti, D. Gonzalez, P. Gunnellini, J. Haller, A. Hinzmann, A. Karavdina, G. Kasieczka, R. Klanner, R. Kogler, N. Kovalchuk, S. Kurz, V. Kutzner, J. Lange, D. Marconi, J. Multhaup, M. Niedziela, C.E.N. Niemeyer, D. Nowatschin, A. Perieanu, A. Reimers, O. Rieger, C. Scharf, P. Schleper, S. Schumann, J. Schwandt, J. Sonneveld, H. Stadie, G. Steinbrück, F.M. Stober, M. Stöver, B. Vormwald, I. Zoi

University of Hamburg, Hamburg, Germany

M. Akbiyik, C. Barth, M. Baselga, S. Baur, E. Butz, R. Caspart, T. Chwalek, F. Colombo, W. De Boer, A. Dierlamm, K. El Morabit, N. Faltermann, B. Freund, M. Giffels, M.A. Harrendorf, F. Hartmann [17], S.M. Heindl, U. Husemann, I. Katkov [15], S. Kudella, S. Mitra, M.U. Mozer, Th. Müller, M. Musich, M. Plagge, G. Quast, K. Rabbertz, M. Schröder, I. Shvetsov, H.J. Simonis, R. Ulrich, S. Wayand, M. Weber, T. Weiler, C. Wöhrmann, R. Wolf

Karlsruher Institut fuer Technologie, Karlsruhe, Germany

G. Anagnostou, G. Daskalakis, T. Geralis, A. Kyriakis, D. Loukas, G. Paspalaki

Institute of Nuclear and Particle Physics (INPP), NCSR Demokritos, Aghia Paraskevi, Greece

A. Agapitos, G. Karathanasis, P. Kontaxakis, A. Panagiotou, I. Papavergou, N. Saoulidou, E. Tziaferi, K. Vellidis

National and Kapodistrian University of Athens, Athens, Greece

K. Kousouris, I. Papakrivopoulos, G. Tsipolitis

National Technical University of Athens, Athens, Greece

I. Evangelou, C. Foudas, P. Gianneios, P. Katsoulis, P. Kokkas, S. Mallios, N. Manthos, I. Papadopoulos, E. Paradas, J. Strologas, F.A. Triantis, D. Tsitsonis

University of Ioánnina, Ioánnina, Greece

M. Bartók [21], M. Csanad, N. Filipovic, P. Major, M.I. Nagy, G. Pasztor, O. Surányi, G.I. Veres

MTA-ELTE Lendület CMS Particle and Nuclear Physics Group, Eötvös Loránd University, Budapest, Hungary

G. Bencze, C. Hajdu, D. Horvath [22], Á. Hunyadi, F. Sikler, T.Á. Vámi, V. Veszpremi, G. Vesztergombi [†]

Wigner Research Centre for Physics, Budapest, Hungary

N. Beni, S. Czellar, J. Karancsi [21], A. Makovec, J. Molnar, Z. Szillasi

Institute of Nuclear Research ATOMKI, Debrecen, Hungary

P. Raics, Z.L. Trocsanyi, B. Ujvari

Institute of Physics, University of Debrecen, Debrecen, Hungary

S. Choudhury, J.R. Komaragiri, P.C. Tiwari

Indian Institute of Science (IISc), Bangalore, India

S. Bahinipati [24], C. Kar, P. Mal, K. Mandal, A. Nayak [25], S. Roy Chowdhury, D.K. Sahoo [24], S.K. Swain

National Institute of Science Education and Research, HBNI, Bhubaneswar, India

S. Bansal, S.B. Beri, V. Bhatnagar, S. Chauhan, R. Chawla, N. Dhingra, R. Gupta, A. Kaur, M. Kaur, S. Kaur, P. Kumari, M. Lohan, M. Meena, A. Mehta, K. Sandeep, S. Sharma, J.B. Singh, A.K. Virdi, G. Walia

Panjab University, Chandigarh, India

A. Bhardwaj, B.C. Choudhary, R.B. Garg, M. Gola, S. Keshri, Ashok Kumar, S. Malhotra, M. Naimuddin, P. Priyanka, K. Ranjan, Aashaq Shah, R. Sharma

University of Delhi, Delhi, India

R. Bhardwaj [26], M. Bharti [26], R. Bhattacharya, S. Bhattacharya, U. Bhawandeep [26], D. Bhowmik, S. Dey, S. Dutt [26], S. Dutta, S. Ghosh, K. Mondal, S. Nandan, A. Purohit, P.K. Rout, A. Roy, G. Saha, S. Sarkar, M. Sharan, B. Singh [26], S. Thakur [26]

Saha Institute of Nuclear Physics, HBNI, Kolkata, India

P.K. Behera, A. Muhammad

Indian Institute of Technology Madras, Madras, India

R. Chudasama, D. Dutta, V. Jha, V. Kumar, D.K. Mishra, P.K. Netrakanti, L.M. Pant, P. Shukla

Bhabha Atomic Research Centre, Mumbai, India

T. Aziz, M.A. Bhat, S. Dugad, G.B. Mohanty, N. Sur, B. Sutar, Ravindra Kumar Verma

Tata Institute of Fundamental Research-A, Mumbai, India

S. Banerjee, S. Bhattacharya, S. Chatterjee, P. Das, M. Guchait, Sa. Jain, S. Karmakar, S. Kumar, M. Maity [27], G. Majumder, K. Mazumdar, N. Sahoo, T. Sarkar [27]

Tata Institute of Fundamental Research-B, Mumbai, India

S. Chauhan, S. Dube, V. Hegde, A. Kapoor, K. Kothekar, S. Pandey, A. Rane, A. Rastogi, S. Sharma

Indian Institute of Science Education and Research (IISER), Pune, India

S. Chenarani [28], E. Eskandari Tadavani, S.M. Etesami [28], M. Khakzad, M. Mohammadi Najafabadi, M. Naseri, F. Rezaei Hosseinabadi, B. Safarzadeh [29], M. Zeinali

Institute for Research in Fundamental Sciences (IPM), Tehran, Iran

M. Felcini, M. Grunewald

University College Dublin, Dublin, Ireland

M. Abbrescia [a,b], C. Calabria [a,b], A. Colaleo [a], D. Creanza [a,c], L. Cristella [a,b], N. De Filippis [a,c], M. De Palma [a,b], A. Di Florio [a,b], F. Errico [a,b], L. Fiore [a], A. Gelmi [a,b], G. Iaselli [a,c], M. Ince [a,b], S. Lezki [a,b], G. Maggi [a,c], M. Maggi [a], G. Miniello [a,b], S. My [a,b], S. Nuzzo [a,b], A. Pompili [a,b], G. Pugliese [a,c], R. Radogna [a], A. Ranieri [a], G. Selvaggi [a,b], A. Sharma [a], L. Silvestris [a], R. Venditti [a], P. Verwilligen [a]

[a] *INFN Sezione di Bari, Bari, Italy*
[b] *Università di Bari, Bari, Italy*
[c] *Politecnico di Bari, Bari, Italy*

G. Abbiendi [a], C. Battilana [a,b], D. Bonacorsi [a,b], L. Borgonovi [a,b], S. Braibant-Giacomelli [a,b], R. Campanini [a,b], P. Capiluppi [a,b], A. Castro [a,b], F.R. Cavallo [a], S.S. Chhibra [a,b], G. Codispoti [a,b], M. Cuffiani [a,b], G.M. Dallavalle [a], F. Fabbri [a], A. Fanfani [a,b], E. Fontanesi, P. Giacomelli [a], C. Grandi [a], L. Guiducci [a,b], F. Iemmi [a,b], S. Lo Meo [a], S. Marcellini [a], G. Masetti [a], A. Montanari [a], F.L. Navarria [a,b], A. Perrotta [a], F. Primavera [a,b,17], A.M. Rossi [a,b], T. Rovelli [a,b], G.P. Siroli [a,b], N. Tosi [a]

[a] *INFN Sezione di Bologna, Bologna, Italy*
[b] *Università di Bologna, Bologna, Italy*

S. Albergo [a,b], A. Di Mattia [a], R. Potenza [a,b], A. Tricomi [a,b], C. Tuve [a,b]

[a] *INFN Sezione di Catania, Catania, Italy*
[b] *Università di Catania, Catania, Italy*

G. Barbagli [a], K. Chatterjee [a,b], V. Ciulli [a,b], C. Civinini [a], R. D'Alessandro [a,b], E. Focardi [a,b], G. Latino, P. Lenzi [a,b], M. Meschini [a], S. Paoletti [a], L. Russo [a,30], G. Sguazzoni [a], D. Strom [a], L. Viliani [a]

[a] *INFN Sezione di Firenze, Firenze, Italy*
[b] *Università di Firenze, Firenze, Italy*

L. Benussi, S. Bianco, F. Fabbri, D. Piccolo

INFN Laboratori Nazionali di Frascati, Frascati, Italy

F. Ferro [a], R. Mulargia [a,b], F. Ravera [a,b], E. Robutti [a], S. Tosi [a,b]

[a] *INFN Sezione di Genova, Genova, Italy*
[b] *Università di Genova, Genova, Italy*

A. Benaglia [a], A. Beschi [b], F. Brivio [a,b], V. Ciriolo [a,b,17], S. Di Guida [a,b,17], M.E. Dinardo [a,b], S. Fiorendi [a,b], S. Gennai [a], A. Ghezzi [a,b], P. Govoni [a,b], M. Malberti [a,b], S. Malvezzi [a], D. Menasce [a], F. Monti, L. Moroni [a], M. Paganoni [a,b], D. Pedrini [a], S. Ragazzi [a,b], T. Tabarelli de Fatis [a,b], D. Zuolo [a,b]

[a] *INFN Sezione di Milano-Bicocca, Milano, Italy*
[b] *Università di Milano-Bicocca, Milano, Italy*

S. Buontempo [a], N. Cavallo [a,c], A. De Iorio [a,b], A. Di Crescenzo [a,b], F. Fabozzi [a,c], F. Fienga [a], G. Galati [a], A.O.M. Iorio [a,b], W.A. Khan [a], L. Lista [a], S. Meola [a,d,17], P. Paolucci [a,17], C. Sciacca [a,b], E. Voevodina [a,b]

[a] *INFN Sezione di Napoli, Napoli, Italy*
[b] *Università di Napoli 'Federico II', Napoli, Italy*
[c] *Università della Basilicata, Potenza, Italy*
[d] *Università G. Marconi, Roma, Italy*

P. Azzi [a], N. Bacchetta [a], D. Bisello [a,b], A. Boletti [a,b], A. Bragagnolo, R. Carlin [a,b], P. Checchia [a], M. Dall'Osso [a,b], P. De Castro Manzano [a], T. Dorigo [a], U. Dosselli [a], F. Gasparini [a,b], U. Gasparini [a,b], A. Gozzelino [a], S.Y. Hoh, S. Lacaprara [a], P. Lujan, M. Margoni [a,b], A.T. Meneguzzo [a,b], J. Pazzini [a,b], M. Presilla [b], P. Ronchese [a,b], R. Rossin [a,b], F. Simonetto [a,b], A. Tiko, E. Torassa [a], M. Tosi [a,b], M. Zanetti [a,b], P. Zotto [a,b], G. Zumerle [a,b]

[a] INFN Sezione di Padova, Padova, Italy
[b] Università di Padova, Padova, Italy
[c] Università di Trento, Trento, Italy

A. Braghieri [a], A. Magnani [a], P. Montagna [a,b], S.P. Ratti [a,b], V. Re [a], M. Ressegotti [a,b], C. Riccardi [a,b], P. Salvini [a], I. Vai [a,b], P. Vitulo [a,b]

[a] INFN Sezione di Pavia, Pavia, Italy
[b] Università di Pavia, Pavia, Italy

M. Biasini [a,b], G.M. Bilei [a], C. Cecchi [a,b], D. Ciangottini [a,b], L. Fanò [a,b], P. Lariccia [a,b], R. Leonardi [a,b], E. Manoni [a], G. Mantovani [a,b], V. Mariani [a,b], M. Menichelli [a], A. Rossi [a,b], A. Santocchia [a,b], D. Spiga [a]

[a] INFN Sezione di Perugia, Perugia, Italy
[b] Università di Perugia, Perugia, Italy

K. Androsov [a], P. Azzurri [a], G. Bagliesi [a], L. Bianchini [a], T. Boccali [a], L. Borrello, R. Castaldi [a], M.A. Ciocci [a,b], R. Dell'Orso [a], G. Fedi [a], F. Fiori [a,c], L. Giannini [a,c], A. Giassi [a], M.T. Grippo [a], F. Ligabue [a,c], E. Manca [a,c], G. Mandorli [a,c], A. Messineo [a,b], F. Palla [a], A. Rizzi [a,b], G. Rolandi [31], P. Spagnolo [a], R. Tenchini [a], G. Tonelli [a,b], A. Venturi [a], P.G. Verdini [a]

[a] INFN Sezione di Pisa, Pisa, Italy
[b] Università di Pisa, Pisa, Italy
[c] Scuola Normale Superiore di Pisa, Pisa, Italy

L. Barone [a,b], F. Cavallari [a], M. Cipriani [a,b], D. Del Re [a,b], E. Di Marco [a,b], M. Diemoz [a], S. Gelli [a,b], E. Longo [a,b], B. Marzocchi [a,b], P. Meridiani [a], G. Organtini [a,b], F. Pandolfi [a], R. Paramatti [a,b], F. Preiato [a,b], S. Rahatlou [a,b], C. Rovelli [a], F. Santanastasio [a,b]

[a] INFN Sezione di Roma, Rome, Italy
[b] Sapienza Università di Roma, Rome, Italy

N. Amapane [a,b], R. Arcidiacono [a,c], S. Argiro [a,b], M. Arneodo [a,c], N. Bartosik [a], R. Bellan [a,b], C. Biino [a], A. Cappati [a,b], N. Cartiglia [a], F. Cenna [a,b], S. Cometti [a], M. Costa [a,b], R. Covarelli [a,b], N. Demaria [a], B. Kiani [a,b], C. Mariotti [a], S. Maselli [a], E. Migliore [a,b], V. Monaco [a,b], E. Monteil [a,b], M. Monteno [a], M.M. Obertino [a,b], L. Pacher [a,b], N. Pastrone [a], M. Pelliccioni [a], G.L. Pinna Angioni [a,b], A. Romero [a,b], M. Ruspa [a,c], R. Sacchi [a,b], R. Salvatico [a,b], K. Shchelina [a,b], V. Sola [a], A. Solano [a,b], D. Soldi [a,b], A. Staiano [a]

[a] INFN Sezione di Torino, Torino, Italy
[b] Università di Torino, Torino, Italy
[c] Università del Piemonte Orientale, Novara, Italy

S. Belforte [a], V. Candelise [a,b], M. Casarsa [a], F. Cossutti [a], A. Da Rold [a,b], G. Della Ricca [a,b], F. Vazzoler [a,b], A. Zanetti [a]

[a] INFN Sezione di Trieste, Trieste, Italy
[b] Università di Trieste, Trieste, Italy

D.H. Kim, G.N. Kim, M.S. Kim, J. Lee, S. Lee, S.W. Lee, C.S. Moon, Y.D. Oh, S.I. Pak, S. Sekmen, D.C. Son, Y.C. Yang

Kyungpook National University, Daegu, Republic of Korea

H. Kim, D.H. Moon, G. Oh

Chonnam National University, Institute for Universe and Elementary Particles, Kwangju, Republic of Korea

B. Francois, J. Goh [32], T.J. Kim

Hanyang University, Seoul, Republic of Korea

S. Cho, S. Choi, Y. Go, D. Gyun, S. Ha, B. Hong, Y. Jo, K. Lee, K.S. Lee, S. Lee, J. Lim, S.K. Park, Y. Roh

Korea University, Seoul, Republic of Korea

H.S. Kim

Sejong University, Seoul, Republic of Korea

J. Almond, J. Kim, J.S. Kim, H. Lee, K. Lee, K. Nam, S.B. Oh, B.C. Radburn-Smith, S.h. Seo, U.K. Yang, H.D. Yoo, G.B. Yu

Seoul National University, Seoul, Republic of Korea

D. Jeon, H. Kim, J.H. Kim, J.S.H. Lee, I.C. Park

University of Seoul, Seoul, Republic of Korea

Y. Choi, C. Hwang, J. Lee, I. Yu

Sungkyunkwan University, Suwon, Republic of Korea

V. Dudenas, A. Juodagalvis, J. Vaitkus

Vilnius University, Vilnius, Lithuania

I. Ahmed, Z.A. Ibrahim, M.A.B. Md Ali [33], F. Mohamad Idris [34], W.A.T. Wan Abdullah, M.N. Yusli, Z. Zolkapli

National Centre for Particle Physics, Universiti Malaya, Kuala Lumpur, Malaysia

J.F. Benitez, A. Castaneda Hernandez, J.A. Murillo Quijada

Universidad de Sonora (UNISON), Hermosillo, Mexico

H. Castilla-Valdez, E. De La Cruz-Burelo, M.C. Duran-Osuna, I. Heredia-De La Cruz [35], R. Lopez-Fernandez, J. Mejia Guisao, R.I. Rabadan-Trejo, M. Ramirez-Garcia, G. Ramirez-Sanchez, R. Reyes-Almanza, A. Sanchez-Hernandez

Centro de Investigacion y de Estudios Avanzados del IPN, Mexico City, Mexico

S. Carrillo Moreno, C. Oropeza Barrera, F. Vazquez Valencia

Universidad Iberoamericana, Mexico City, Mexico

J. Eysermans, I. Pedraza, H.A. Salazar Ibarguen, C. Uribe Estrada

Benemerita Universidad Autonoma de Puebla, Puebla, Mexico

A. Morelos Pineda

Universidad Autónoma de San Luis Potosí, San Luis Potosí, Mexico

D. Krofcheck

University of Auckland, Auckland, New Zealand

S. Bheesette, P.H. Butler

University of Canterbury, Christchurch, New Zealand

A. Ahmad, M. Ahmad, M.I. Asghar, Q. Hassan, H.R. Hoorani, A. Saddique, M.A. Shah, M. Shoaib, M. Waqas

National Centre for Physics, Quaid-I-Azam University, Islamabad, Pakistan

H. Bialkowska, M. Bluj, B. Boimska, T. Frueboes, M. Górski, M. Kazana, M. Szleper, P. Traczyk, P. Zalewski

National Centre for Nuclear Research, Swierk, Poland

K. Bunkowski, A. Byszuk [36], K. Doroba, A. Kalinowski, M. Konecki, J. Krolikowski, M. Misiura, M. Olszewski, A. Pyskir, M. Walczak

Institute of Experimental Physics, Faculty of Physics, University of Warsaw, Warsaw, Poland

M. Araujo, P. Bargassa, C. Beirão Da Cruz E Silva, A. Di Francesco, P. Faccioli, B. Galinhas, M. Gallinaro, J. Hollar, N. Leonardo, J. Seixas, G. Strong, O. Toldaiev, J. Varela

Laboratório de Instrumentação e Física Experimental de Partículas, Lisboa, Portugal

S. Afanasiev, P. Bunin, M. Gavrilenko, I. Golutvin, I. Gorbunov, A. Kamenev, V. Karjavine, A. Lanev, A. Malakhov, V. Matveev [37,38], P. Moisenz, V. Palichik, V. Perelygin, S. Shmatov, S. Shulha, N. Skatchkov, V. Smirnov, N. Voytishin, A. Zarubin

Joint Institute for Nuclear Research, Dubna, Russia

V. Golovtsov, Y. Ivanov, V. Kim [39], E. Kuznetsova [40], P. Levchenko, V. Murzin, V. Oreshkin, I. Smirnov, D. Sosnov, V. Sulimov, L. Uvarov, S. Vavilov, A. Vorobyev

Petersburg Nuclear Physics Institute, Gatchina (St. Petersburg), Russia

Yu. Andreev, A. Dermenev, S. Gninenko, N. Golubev, A. Karneyeu, M. Kirsanov, N. Krasnikov, A. Pashenkov, D. Tlisov, A. Toropin

Institute for Nuclear Research, Moscow, Russia

V. Epshteyn, V. Gavrilov, N. Lychkovskaya, V. Popov, I. Pozdnyakov, G. Safronov, A. Spiridonov, A. Stepennov, V. Stolin, M. Toms, E. Vlasov, A. Zhokin

Institute for Theoretical and Experimental Physics, Moscow, Russia

T. Aushev

Moscow Institute of Physics and Technology, Moscow, Russia

M. Chadeeva [41], P. Parygin, D. Philippov, S. Polikarpov [41], E. Popova, V. Rusinov

National Research Nuclear University 'Moscow Engineering Physics Institute' (MEPhI), Moscow, Russia

V. Andreev, M. Azarkin, I. Dremin [38], M. Kirakosyan, A. Terkulov

P.N. Lebedev Physical Institute, Moscow, Russia

A. Baskakov, A. Belyaev, E. Boos, M. Dubinin [42], L. Dudko, A. Ershov, A. Gribushin, V. Klyukhin, O. Kodolova, I. Lokhtin, I. Miagkov, S. Obraztsov, S. Petrushanko, V. Savrin, A. Snigirev

Skobeltsyn Institute of Nuclear Physics, Lomonosov Moscow State University, Moscow, Russia

A. Barnyakov [43], V. Blinov [43], T. Dimova [43], L. Kardapoltsev [43], Y. Skovpen [43]

Novosibirsk State University (NSU), Novosibirsk, Russia

I. Azhgirey, I. Bayshev, S. Bitioukov, V. Kachanov, A. Kalinin, D. Konstantinov, P. Mandrik, V. Petrov, R. Ryutin, S. Slabospitskii, A. Sobol, S. Troshin, N. Tyurin, A. Uzunian, A. Volkov

Institute for High Energy Physics of National Research Centre 'Kurchatov Institute', Protvino, Russia

A. Babaev, S. Baidali, V. Okhotnikov

National Research Tomsk Polytechnic University, Tomsk, Russia

P. Adzic [44], P. Cirkovic, D. Devetak, M. Dordevic, J. Milosevic

University of Belgrade, Faculty of Physics and Vinca Institute of Nuclear Sciences, Belgrade, Serbia

J. Alcaraz Maestre, A. Álvarez Fernández, I. Bachiller, M. Barrio Luna, J.A. Brochero Cifuentes, M. Cerrada, N. Colino, B. De La Cruz, A. Delgado Peris, C. Fernandez Bedoya, J.P. Fernández Ramos, J. Flix, M.C. Fouz,

O. Gonzalez Lopez, S. Goy Lopez, J.M. Hernandez, M.I. Josa, D. Moran, A. Pérez-Calero Yzquierdo, J. Puerta Pelayo, I. Redondo, L. Romero, S. Sánchez Navas, M.S. Soares, A. Triossi

Centro de Investigaciones Energéticas Medioambientales y Tecnológicas (CIEMAT), Madrid, Spain

C. Albajar, J.F. de Trocóniz

Universidad Autónoma de Madrid, Madrid, Spain

J. Cuevas, C. Erice, J. Fernandez Menendez, S. Folgueras, I. Gonzalez Caballero, J.R. González Fernández, E. Palencia Cortezon, V. Rodríguez Bouza, S. Sanchez Cruz, J.M. Vizan Garcia

Universidad de Oviedo, Oviedo, Spain

I.J. Cabrillo, A. Calderon, B. Chazin Quero, J. Duarte Campderros, M. Fernandez, P.J. Fernández Manteca, A. García Alonso, J. Garcia-Ferrero, G. Gomez, A. Lopez Virto, J. Marco, C. Martinez Rivero, P. Martinez Ruiz del Arbol, F. Matorras, J. Piedra Gomez, C. Prieels, T. Rodrigo, A. Ruiz-Jimeno, L. Scodellaro, N. Trevisani, I. Vila, R. Vilar Cortabitarte

Instituto de Física de Cantabria (IFCA), CSIC-Universidad de Cantabria, Santander, Spain

N. Wickramage

University of Ruhuna, Department of Physics, Matara, Sri Lanka

D. Abbaneo, B. Akgun, E. Auffray, G. Auzinger, P. Baillon, A.H. Ball, D. Barney, J. Bendavid, M. Bianco, A. Bocci, C. Botta, E. Brondolin, T. Camporesi, M. Cepeda, G. Cerminara, E. Chapon, Y. Chen, G. Cucciati, D. d'Enterria, A. Dabrowski, N. Daci, V. Daponte, A. David, A. De Roeck, N. Deelen, M. Dobson, M. Dünser, N. Dupont, A. Elliott-Peisert, P. Everaerts, F. Fallavollita [45], D. Fasanella, G. Franzoni, J. Fulcher, W. Funk, D. Gigi, A. Gilbert, K. Gill, F. Glege, M. Gruchala, M. Guilbaud, D. Gulhan, J. Hegeman, C. Heidegger, V. Innocente, A. Jafari, P. Janot, O. Karacheban [20], J. Kieseler, A. Kornmayer, M. Krammer [1], C. Lange, P. Lecoq, C. Lourenço, L. Malgeri, M. Mannelli, A. Massironi, F. Meijers, J.A. Merlin, S. Mersi, E. Meschi, P. Milenovic [46], F. Moortgat, M. Mulders, J. Ngadiuba, S. Nourbakhsh, S. Orfanelli, L. Orsini, F. Pantaleo [17], L. Pape, E. Perez, M. Peruzzi, A. Petrilli, G. Petrucciani, A. Pfeiffer, M. Pierini, F.M. Pitters, D. Rabady, A. Racz, T. Reis, M. Rovere, H. Sakulin, C. Schäfer, C. Schwick, M. Selvaggi, A. Sharma, P. Silva, P. Sphicas [47], A. Stakia, J. Steggemann, D. Treille, A. Tsirou, V. Veckalns [48], M. Verzetti, W.D. Zeuner

CERN, European Organization for Nuclear Research, Geneva, Switzerland

L. Caminada [49], K. Deiters, W. Erdmann, R. Horisberger, Q. Ingram, H.C. Kaestli, D. Kotlinski, U. Langenegger, T. Rohe, S.A. Wiederkehr

Paul Scherrer Institut, Villigen, Switzerland

M. Backhaus, L. Bäni, P. Berger, N. Chernyavskaya, G. Dissertori, M. Dittmar, M. Donegà, C. Dorfer, T.A. Gómez Espinosa, C. Grab, D. Hits, T. Klijnsma, W. Lustermann, R.A. Manzoni, M. Marionneau, M.T. Meinhard, F. Micheli, P. Musella, F. Nessi-Tedaldi, J. Pata, F. Pauss, G. Perrin, L. Perrozzi, S. Pigazzini, M. Quittnat, C. Reissel, D. Ruini, D.A. Sanz Becerra, M. Schönenberger, L. Shchutska, V.R. Tavolaro, K. Theofilatos, M.L. Vesterbacka Olsson, R. Wallny, D.H. Zhu

ETH Zurich – Institute for Particle Physics and Astrophysics (IPA), Zurich, Switzerland

T.K. Aarrestad, C. Amsler [50], D. Brzhechko, M.F. Canelli, A. De Cosa, R. Del Burgo, S. Donato, C. Galloni, T. Hreus, B. Kilminster, S. Leontsinis, I. Neutelings, G. Rauco, P. Robmann, D. Salerno, K. Schweiger, C. Seitz, Y. Takahashi, A. Zucchetta

Universität Zürich, Zurich, Switzerland

T.H. Doan, R. Khurana, C.M. Kuo, W. Lin, A. Pozdnyakov, S.S. Yu

National Central University, Chung-Li, Taiwan

P. Chang, Y. Chao, K.F. Chen, P.H. Chen, W.-S. Hou, Y.F. Liu, R.-S. Lu, E. Paganis, A. Psallidas, A. Steen

National Taiwan University (NTU), Taipei, Taiwan

B. Asavapibhop, N. Srimanobhas, N. Suwonjandee

Chulalongkorn University, Faculty of Science, Department of Physics, Bangkok, Thailand

A. Bat, F. Boran, S. Cerci [51], S. Damarseckin, Z.S. Demiroglu, F. Dolek, C. Dozen, I. Dumanoglu, E. Eskut, S. Girgis, G. Gokbulut, Y. Guler, E. Gurpinar, I. Hos [52], C. Isik, E.E. Kangal [53], O. Kara, A. Kayis Topaksu, U. Kiminsu, M. Oglakci, G. Onengut, K. Ozdemir [54], D. Sunar Cerci [51], B. Tali [51], U.G. Tok, S. Turkcapar, I.S. Zorbakir, C. Zorbilmez

Çukurova University, Physics Department, Science and Art Faculty, Adana, Turkey

B. Isildak [55], G. Karapinar [56], M. Yalvac, M. Zeyrek

Middle East Technical University, Physics Department, Ankara, Turkey

I.O. Atakisi, E. Gülmez, M. Kaya [57], O. Kaya [58], S. Ozkorucuklu [59], S. Tekten, E.A. Yetkin [60]

Bogazici University, Istanbul, Turkey

M.N. Agaras, A. Cakir, K. Cankocak, Y. Komurcu, S. Sen [61]

Istanbul Technical University, Istanbul, Turkey

B. Grynyov

Institute for Scintillation Materials of National Academy of Science of Ukraine, Kharkov, Ukraine

L. Levchuk

National Scientific Center, Kharkov Institute of Physics and Technology, Kharkov, Ukraine

F. Ball, J.J. Brooke, D. Burns, E. Clement, D. Cussans, O. Davignon, H. Flacher, J. Goldstein, G.P. Heath, H.F. Heath, L. Kreczko, D.M. Newbold [62], S. Paramesvaran, B. Penning, T. Sakuma, D. Smith, V.J. Smith, J. Taylor, A. Titterton

University of Bristol, Bristol, United Kingdom

K.W. Bell, A. Belyaev [63], C. Brew, R.M. Brown, D. Cieri, D.J.A. Cockerill, J.A. Coughlan, K. Harder, S. Harper, J. Linacre, K. Manolopoulos, E. Olaiya, D. Petyt, C.H. Shepherd-Themistocleous, A. Thea, I.R. Tomalin, T. Williams, W.J. Womersley

Rutherford Appleton Laboratory, Didcot, United Kingdom

R. Bainbridge, P. Bloch, J. Borg, S. Breeze, O. Buchmuller, A. Bundock, D. Colling, P. Dauncey, G. Davies, M. Della Negra, R. Di Maria, G. Hall, G. Iles, T. James, M. Komm, C. Laner, L. Lyons, A.-M. Magnan, S. Malik, A. Martelli, J. Nash [64], A. Nikitenko [7], V. Palladino, M. Pesaresi, D.M. Raymond, A. Richards, A. Rose, E. Scott, C. Seez, A. Shtipliyski, G. Singh, M. Stoye, T. Strebler, S. Summers, A. Tapper, K. Uchida, T. Virdee [17], N. Wardle, D. Winterbottom, J. Wright, S.C. Zenz

Imperial College, London, United Kingdom

J.E. Cole, P.R. Hobson, A. Khan, P. Kyberd, C.K. Mackay, A. Morton, I.D. Reid, L. Teodorescu, S. Zahid

Brunel University, Uxbridge, United Kingdom

K. Call, J. Dittmann, K. Hatakeyama, H. Liu, C. Madrid, B. McMaster, N. Pastika, C. Smith

Baylor University, Waco, USA

R. Bartek, A. Dominguez

Catholic University of America, Washington, DC, USA

A. Buccilli, S.I. Cooper, C. Henderson, P. Rumerio, C. West

The University of Alabama, Tuscaloosa, USA

D. Arcaro, T. Bose, D. Gastler, D. Pinna, D. Rankin, C. Richardson, J. Rohlf, L. Sulak, D. Zou

Boston University, Boston, USA

G. Benelli, X. Coubez, D. Cutts, M. Hadley, J. Hakala, U. Heintz, J.M. Hogan [65], K.H.M. Kwok, E. Laird, G. Landsberg, J. Lee, Z. Mao, M. Narain, S. Sagir [66], R. Syarif, E. Usai, D. Yu

Brown University, Providence, USA

R. Band, C. Brainerd, R. Breedon, D. Burns, M. Calderon De La Barca Sanchez, M. Chertok, J. Conway, R. Conway, P.T. Cox, R. Erbacher, C. Flores, G. Funk, W. Ko, O. Kukral, R. Lander, M. Mulhearn, D. Pellett, J. Pilot, S. Shalhout, M. Shi, D. Stolp, D. Taylor, K. Tos, M. Tripathi, Z. Wang, F. Zhang

University of California, Davis, Davis, USA

M. Bachtis, C. Bravo, R. Cousins, A. Dasgupta, A. Florent, J. Hauser, M. Ignatenko, N. Mccoll, S. Regnard, D. Saltzberg, C. Schnaible, V. Valuev

University of California, Los Angeles, USA

E. Bouvier, K. Burt, R. Clare, J.W. Gary, S.M.A. Ghiasi Shirazi, G. Hanson, G. Karapostoli, E. Kennedy, F. Lacroix, O.R. Long, M. Olmedo Negrete, M.I. Paneva, W. Si, L. Wang, H. Wei, S. Wimpenny, B.R. Yates

University of California, Riverside, Riverside, USA

J.G. Branson, P. Chang, S. Cittolin, M. Derdzinski, R. Gerosa, D. Gilbert, B. Hashemi, A. Holzner, D. Klein, G. Kole, V. Krutelyov, J. Letts, M. Masciovecchio, D. Olivito, S. Padhi, M. Pieri, M. Sani, V. Sharma, S. Simon, M. Tadel, A. Vartak, S. Wasserbaech [67], J. Wood, F. Würthwein, A. Yagil, G. Zevi Della Porta

University of California, San Diego, La Jolla, USA

N. Amin, R. Bhandari, C. Campagnari, M. Citron, V. Dutta, M. Franco Sevilla, L. Gouskos, R. Heller, J. Incandela, H. Mei, A. Ovcharova, H. Qu, J. Richman, D. Stuart, I. Suarez, S. Wang, J. Yoo

University of California, Santa Barbara – Department of Physics, Santa Barbara, USA

D. Anderson, A. Bornheim, J.M. Lawhorn, N. Lu, H.B. Newman, T.Q. Nguyen, M. Spiropulu, J.R. Vlimant, R. Wilkinson, S. Xie, Z. Zhang, R.Y. Zhu

California Institute of Technology, Pasadena, USA

M.B. Andrews, T. Ferguson, T. Mudholkar, M. Paulini, M. Sun, I. Vorobiev, M. Weinberg

Carnegie Mellon University, Pittsburgh, USA

J.P. Cumalat, W.T. Ford, F. Jensen, A. Johnson, E. MacDonald, T. Mulholland, R. Patel, A. Perloff, K. Stenson, K.A. Ulmer, S.R. Wagner

University of Colorado Boulder, Boulder, USA

J. Alexander, J. Chaves, Y. Cheng, J. Chu, A. Datta, K. Mcdermott, N. Mirman, J.R. Patterson, D. Quach, A. Rinkevicius, A. Ryd, L. Skinnari, L. Soffi, S.M. Tan, Z. Tao, J. Thom, J. Tucker, P. Wittich, M. Zientek

Cornell University, Ithaca, USA

S. Abdullin, M. Albrow, M. Alyari, G. Apollinari, A. Apresyan, A. Apyan, S. Banerjee, L.A.T. Bauerdick, A. Beretvas, J. Berryhill, P.C. Bhat, K. Burkett, J.N. Butler, A. Canepa, G.B. Cerati, H.W.K. Cheung, F. Chlebana, M. Cremonesi, J. Duarte, V.D. Elvira, J. Freeman, Z. Gecse, E. Gottschalk, L. Gray, D. Green,

S. Grünendahl, O. Gutsche, J. Hanlon, R.M. Harris, S. Hasegawa, J. Hirschauer, Z. Hu, B. Jayatilaka, S. Jindariani, M. Johnson, U. Joshi, B. Klima, M.J. Kortelainen, B. Kreis, S. Lammel, D. Lincoln, R. Lipton, M. Liu, T. Liu, J. Lykken, K. Maeshima, J.M. Marraffino, D. Mason, P. McBride, P. Merkel, S. Mrenna, S. Nahn, V. O'Dell, K. Pedro, C. Pena, O. Prokofyev, G. Rakness, L. Ristori, A. Savoy-Navarro [68], B. Schneider, E. Sexton-Kennedy, A. Soha, W.J. Spalding, L. Spiegel, S. Stoynev, J. Strait, N. Strobbe, L. Taylor, S. Tkaczyk, N.V. Tran, L. Uplegger, E.W. Vaandering, C. Vernieri, M. Verzocchi, R. Vidal, M. Wang, H.A. Weber, A. Whitbeck

Fermi National Accelerator Laboratory, Batavia, USA

D. Acosta, P. Avery, P. Bortignon, D. Bourilkov, A. Brinkerhoff, L. Cadamuro, A. Carnes, D. Curry, R.D. Field, S.V. Gleyzer, B.M. Joshi, J. Konigsberg, A. Korytov, K.H. Lo, P. Ma, K. Matchev, G. Mitselmakher, D. Rosenzweig, K. Shi, D. Sperka, J. Wang, S. Wang, X. Zuo

University of Florida, Gainesville, USA

Y.R. Joshi, S. Linn

Florida International University, Miami, USA

A. Ackert, T. Adams, A. Askew, S. Hagopian, V. Hagopian, K.F. Johnson, T. Kolberg, G. Martinez, T. Perry, H. Prosper, A. Saha, C. Schiber, R. Yohay

Florida State University, Tallahassee, USA

M.M. Baarmand, V. Bhopatkar, S. Colafranceschi, M. Hohlmann, D. Noonan, M. Rahmani, T. Roy, F. Yumiceva

Florida Institute of Technology, Melbourne, USA

M.R. Adams, L. Apanasevich, D. Berry, R.R. Betts, R. Cavanaugh, X. Chen, S. Dittmer, O. Evdokimov, C.E. Gerber, D.A. Hangal, D.J. Hofman, K. Jung, J. Kamin, C. Mills, M.B. Tonjes, N. Varelas, H. Wang, X. Wang, Z. Wu, J. Zhang

University of Illinois at Chicago (UIC), Chicago, USA

M. Alhusseini, B. Bilki [69], W. Clarida, K. Dilsiz [70], S. Durgut, R.P. Gandrajula, M. Haytmyradov, V. Khristenko, J.-P. Merlo, A. Mestvirishvili, A. Moeller, J. Nachtman, H. Ogul [71], Y. Onel, F. Ozok [72], A. Penzo, C. Snyder, E. Tiras, J. Wetzel

The University of Iowa, Iowa City, USA

B. Blumenfeld, A. Cocoros, N. Eminizer, D. Fehling, L. Feng, A.V. Gritsan, W.T. Hung, P. Maksimovic, J. Roskes, U. Sarica, M. Swartz, M. Xiao, C. You

Johns Hopkins University, Baltimore, USA

A. Al-bataineh, P. Baringer, A. Bean, S. Boren, J. Bowen, A. Bylinkin, J. Castle, S. Khalil, A. Kropivnitskaya, D. Majumder, W. Mcbrayer, M. Murray, C. Rogan, S. Sanders, E. Schmitz, J.D. Tapia Takaki, Q. Wang

The University of Kansas, Lawrence, USA

S. Duric, A. Ivanov, K. Kaadze, D. Kim, Y. Maravin, D.R. Mendis, T. Mitchell, A. Modak, A. Mohammadi

Kansas State University, Manhattan, USA

F. Rebassoo, D. Wright

Lawrence Livermore National Laboratory, Livermore, USA

A. Baden, O. Baron, A. Belloni, S.C. Eno, Y. Feng, C. Ferraioli, N.J. Hadley, S. Jabeen, G.Y. Jeng, R.G. Kellogg, J. Kunkle, A.C. Mignerey, S. Nabili, F. Ricci-Tam, M. Seidel, Y.H. Shin, A. Skuja, S.C. Tonwar, K. Wong

University of Maryland, College Park, USA

D. Abercrombie, B. Allen, V. Azzolini, A. Baty, G. Bauer, R. Bi, S. Brandt, W. Busza, I.A. Cali, J. Curti, M. D'Alfonso, Z. Demiragli, G. Gomez Ceballos, M. Goncharov, P. Harris, D. Hsu, M. Hu, Y. Iiyama, G.M. Innocenti, M. Klute, D. Kovalskyi, Y.-J. Lee, P.D. Luckey, B. Maier, A.C. Marini, C. Mcginn, C. Mironov, S. Narayanan, X. Niu, C. Paus, C. Roland, G. Roland, Z. Shi, G.S.F. Stephans, K. Sumorok, K. Tatar, D. Velicanu, J. Wang, T.W. Wang, B. Wyslouch

Massachusetts Institute of Technology, Cambridge, USA

A.C. Benvenuti [†], R.M. Chatterjee, A. Evans, P. Hansen, J. Hiltbrand, Sh. Jain, S. Kalafut, M. Krohn, Y. Kubota, Z. Lesko, J. Mans, N. Ruckstuhl, R. Rusack, M.A. Wadud

University of Minnesota, Minneapolis, USA

J.G. Acosta, S. Oliveros

University of Mississippi, Oxford, USA

E. Avdeeva, K. Bloom, D.R. Claes, C. Fangmeier, F. Golf, R. Gonzalez Suarez, R. Kamalieddin, I. Kravchenko, J. Monroy, J.E. Siado, G.R. Snow, B. Stieger

University of Nebraska-Lincoln, Lincoln, USA

A. Godshalk, C. Harrington, I. Iashvili, A. Kharchilava, C. Mclean, D. Nguyen, A. Parker, S. Rappoccio, B. Roozbahani

State University of New York at Buffalo, Buffalo, USA

G. Alverson, E. Barberis, C. Freer, Y. Haddad, A. Hortiangtham, D.M. Morse, T. Orimoto, T. Wamorkar, B. Wang, A. Wisecarver, D. Wood

Northeastern University, Boston, USA

S. Bhattacharya, J. Bueghly, O. Charaf, T. Gunter, K.A. Hahn, N. Odell, M.H. Schmitt, K. Sung, M. Trovato, M. Velasco

Northwestern University, Evanston, USA

R. Bucci, N. Dev, M. Hildreth, K. Hurtado Anampa, C. Jessop, D.J. Karmgard, K. Lannon, W. Li, N. Loukas, N. Marinelli, F. Meng, C. Mueller, Y. Musienko [37], M. Planer, A. Reinsvold, R. Ruchti, P. Siddireddy, G. Smith, S. Taroni, M. Wayne, A. Wightman, M. Wolf, A. Woodard

University of Notre Dame, Notre Dame, USA

J. Alimena, L. Antonelli, B. Bylsma, L.S. Durkin, S. Flowers, B. Francis, C. Hill, W. Ji, T.Y. Ling, W. Luo, B.L. Winer

The Ohio State University, Columbus, USA

S. Cooperstein, P. Elmer, J. Hardenbrook, N. Haubrich, S. Higginbotham, A. Kalogeropoulos, S. Kwan, D. Lange, M.T. Lucchini, J. Luo, D. Marlow, K. Mei, I. Ojalvo, J. Olsen, C. Palmer, P. Piroué, J. Salfeld-Nebgen, D. Stickland, C. Tully

Princeton University, Princeton, USA

S. Malik, S. Norberg

University of Puerto Rico, Mayaguez, USA

A. Barker, V.E. Barnes, S. Das, L. Gutay, M. Jones, A.W. Jung, A. Khatiwada, B. Mahakud, D.H. Miller, N. Neumeister, C.C. Peng, S. Piperov, H. Qiu, J.F. Schulte, J. Sun, F. Wang, R. Xiao, W. Xie

Purdue University, West Lafayette, USA

T. Cheng, J. Dolen, N. Parashar

Purdue University Northwest, Hammond, USA

Z. Chen, K.M. Ecklund, S. Freed, F.J.M. Geurts, M. Kilpatrick, Arun Kumar, W. Li, B.P. Padley, R. Redjimi, J. Roberts, J. Rorie, W. Shi, Z. Tu, A. Zhang

Rice University, Houston, USA

A. Bodek, P. de Barbaro, R. Demina, Y.t. Duh, J.L. Dulemba, C. Fallon, T. Ferbel, M. Galanti, A. Garcia-Bellido, J. Han, O. Hindrichs, A. Khukhunaishvili, E. Ranken, P. Tan, R. Taus

University of Rochester, Rochester, USA

J.P. Chou, Y. Gershtein, E. Halkiadakis, A. Hart, M. Heindl, E. Hughes, S. Kaplan, R. Kunnawalkam Elayavalli, S. Kyriacou, I. Laflotte, A. Lath, R. Montalvo, K. Nash, M. Osherson, H. Saka, S. Salur, S. Schnetzer, D. Sheffield, S. Somalwar, R. Stone, S. Thomas, P. Thomassen

Rutgers, The State University of New Jersey, Piscataway, USA

A.G. Delannoy, J. Heideman, G. Riley, S. Spanier

University of Tennessee, Knoxville, USA

O. Bouhali [73], A. Celik, M. Dalchenko, M. De Mattia, A. Delgado, S. Dildick, R. Eusebi, J. Gilmore, T. Huang, T. Kamon [74], S. Luo, D. Marley, R. Mueller, D. Overton, L. Perniè, D. Rathjens, A. Safonov

Texas A&M University, College Station, USA

N. Akchurin, J. Damgov, F. De Guio, P.R. Dudero, S. Kunori, K. Lamichhane, S.W. Lee, T. Mengke, S. Muthumuni, T. Peltola, S. Undleeb, I. Volobouev, Z. Wang

Texas Tech University, Lubbock, USA

S. Greene, A. Gurrola, R. Janjam, W. Johns, C. Maguire, A. Melo, H. Ni, K. Padeken, F. Romeo, J.D. Ruiz Alvarez, P. Sheldon, S. Tuo, J. Velkovska, M. Verweij, Q. Xu

Vanderbilt University, Nashville, USA

M.W. Arenton, P. Barria, B. Cox, R. Hirosky, M. Joyce, A. Ledovskoy, H. Li, C. Neu, T. Sinthuprasith, Y. Wang, E. Wolfe, F. Xia

University of Virginia, Charlottesville, USA

R. Harr, P.E. Karchin, N. Poudyal, J. Sturdy, P. Thapa, S. Zaleski

Wayne State University, Detroit, USA

J. Buchanan, C. Caillol, D. Carlsmith, S. Dasu, I. De Bruyn, L. Dodd, B. Gomber, M. Grothe, M. Herndon, A. Hervé, U. Hussain, P. Klabbers, A. Lanaro, K. Long, R. Loveless, T. Ruggles, A. Savin, V. Sharma, N. Smith, W.H. Smith, N. Woods

University of Wisconsin – Madison, Madison, WI, USA

† Deceased.
[1] Also at Vienna University of Technology, Vienna, Austria.
[2] Also at IRFU, CEA, Université Paris-Saclay, Gif-sur-Yvette, France.
[3] Also at Universidade Estadual de Campinas, Campinas, Brazil.
[4] Also at Federal University of Rio Grande do Sul, Porto Alegre, Brazil.
[5] Also at Université Libre de Bruxelles, Bruxelles, Belgium.
[6] Also at University of Chinese Academy of Sciences, Beijing, China.
[7] Also at Institute for Theoretical and Experimental Physics, Moscow, Russia.
[8] Also at Joint Institute for Nuclear Research, Dubna, Russia.
[9] Also at Zewail City of Science and Technology, Zewail, Egypt.
[10] Also at Fayoum University, El-Fayoum, Egypt.

[11] Now at British University in Egypt, Cairo, Egypt.
[12] Now at Ain Shams University, Cairo, Egypt.
[13] Also at Department of Physics, King Abdulaziz University, Jeddah, Saudi Arabia.
[14] Also at Université de Haute Alsace, Mulhouse, France.
[15] Also at Skobeltsyn Institute of Nuclear Physics, Lomonosov Moscow State University, Moscow, Russia.
[16] Also at Tbilisi State University, Tbilisi, Georgia.
[17] Also at CERN, European Organization for Nuclear Research, Geneva, Switzerland.
[18] Also at RWTH Aachen University, III. Physikalisches Institut A, Aachen, Germany.
[19] Also at University of Hamburg, Hamburg, Germany.
[20] Also at Brandenburg University of Technology, Cottbus, Germany.
[21] Also at Institute of Physics, University of Debrecen, Debrecen, Hungary.
[22] Also at Institute of Nuclear Research ATOMKI, Debrecen, Hungary.
[23] Also at MTA-ELTE Lendület CMS Particle and Nuclear Physics Group, Eötvös Loránd University, Budapest, Hungary.
[24] Also at Indian Institute of Technology Bhubaneswar, Bhubaneswar, India.
[25] Also at Institute of Physics, Bhubaneswar, India.
[26] Also at Shoolini University, Solan, India.
[27] Also at University of Visva-Bharati, Santiniketan, India.
[28] Also at Isfahan University of Technology, Isfahan, Iran.
[29] Also at Plasma Physics Research Center, Science and Research Branch, Islamic Azad University, Tehran, Iran.
[30] Also at Università degli Studi di Siena, Siena, Italy.
[31] Also at Scuola Normale e Sezione dell'INFN, Pisa, Italy.
[32] Also at Kyunghee University, Seoul, Republic of Korea.
[33] Also at International Islamic University of Malaysia, Kuala Lumpur, Malaysia.
[34] Also at Malaysian Nuclear Agency, MOSTI, Kajang, Malaysia.
[35] Also at Consejo Nacional de Ciencia y Tecnología, Mexico City, Mexico.
[36] Also at Warsaw University of Technology, Institute of Electronic Systems, Warsaw, Poland.
[37] Also at Institute for Nuclear Research, Moscow, Russia.
[38] Now at National Research Nuclear University 'Moscow Engineering Physics Institute' (MEPhI), Moscow, Russia.
[39] Also at St. Petersburg State Polytechnical University, St. Petersburg, Russia.
[40] Also at University of Florida, Gainesville, USA.
[41] Also at P.N. Lebedev Physical Institute, Moscow, Russia.
[42] Also at California Institute of Technology, Pasadena, USA.
[43] Also at Budker Institute of Nuclear Physics, Novosibirsk, Russia.
[44] Also at Faculty of Physics, University of Belgrade, Belgrade, Serbia.
[45] Also at INFN Sezione di Pavia[a], Università di Pavia[b], Pavia, Italy.
[46] Also at University of Belgrade, Faculty of Physics and Vinca Institute of Nuclear Sciences, Belgrade, Serbia.
[47] Also at National and Kapodistrian University of Athens, Athens, Greece.
[48] Also at Riga Technical University, Riga, Latvia.
[49] Also at Universität Zürich, Zurich, Switzerland.
[50] Also at Stefan Meyer Institute for Subatomic Physics (SMI), Vienna, Austria.
[51] Also at Adiyaman University, Adiyaman, Turkey.
[52] Also at Istanbul Aydin University, Istanbul, Turkey.
[53] Also at Mersin University, Mersin, Turkey.
[54] Also at Piri Reis University, Istanbul, Turkey.
[55] Also at Ozyegin University, Istanbul, Turkey.
[56] Also at Izmir Institute of Technology, Izmir, Turkey.
[57] Also at Marmara University, Istanbul, Turkey.
[58] Also at Kafkas University, Kars, Turkey.
[59] Also at Istanbul University, Faculty of Science, Istanbul, Turkey.
[60] Also at Istanbul Bilgi University, Istanbul, Turkey.
[61] Also at Hacettepe University, Ankara, Turkey.
[62] Also at Rutherford Appleton Laboratory, Didcot, United Kingdom.
[63] Also at School of Physics and Astronomy, University of Southampton, Southampton, United Kingdom.
[64] Also at Monash University, Faculty of Science, Clayton, Australia.
[65] Also at Bethel University, St. Paul, USA.
[66] Also at Karamanoğlu Mehmetbey University, Karaman, Turkey.
[67] Also at Utah Valley University, Orem, USA.
[68] Also at Purdue University, West Lafayette, USA.
[69] Also at Beykent University, Istanbul, Turkey.
[70] Also at Bingol University, Bingol, Turkey.
[71] Also at Sinop University, Sinop, Turkey.
[72] Also at Mimar Sinan University, Istanbul, Istanbul, Turkey.
[73] Also at Texas A&M University at Qatar, Doha, Qatar.
[74] Also at Kyungpook National University, Daegu, Republic of Korea.